



A two-step sensitivity analysis for hydrological signatures in Jinhua River Basin, East China

Journal:	<i>Hydrological Sciences Journal</i>
Manuscript ID	HSJ-2016-0405.R2
Manuscript Type:	Original Article
Date Submitted by the Author:	n/a
Complete List of Authors:	Pan, Suli; Zhejiang University, Guangtao, Fu; University of Exeter Chiang, Yen-Ming ; Zhejiang University, Department of Hydraulic Engineering Ran, Qihua; Zhejiang University Xu, Yueping; Zhejiang University, Hydraulic Engineering
Keywords:	sensitivity analysis, ANOVA method, Sobol's method, Hydrological signature, DHSVM, Peak flow

SCHOLARONE™
Manuscripts

Title: A two-step sensitivity analysis for hydrological signatures in Jinhua River Basin, East China

1. Author name and affiliations:

Suli Pan^a, Guangtao Fu^b, Yen-Ming Chiang^a, Qihua Ran^a and Yue-Ping Xu^a

^aInstitute of Hydrology and Water Resources, College of Civil Engineering and Architecture, Zhejiang University, Hangzhou, 310058, China

^bCenter for Water Systems, College of Engineering, Mathematics and Physical Sciences, University of Exeter, North Park Road, Harrison Building, Exeter, EX4 4QF, UK

Full postal address and e-mail address:

Suli Pan:

Postal address: Room B526, Anzhong Building, Campus Zijingang, Zhejiang University, No.388 Yuhangtang Road, Hangzhou, China. **E-mail:** pansuli@zju.edu.cn

Guangtao Fu:

Postal address: Center for Water Systems, College of Engineering, Mathematics and Physical Sciences, University of Exeter, North Park Road, Harrison Building, Exeter, EX4,4QF,UK. **E-mail:** G.Fu@exeter.ac.uk

Yen-Ming Chiang:

Postal address: Room B528, Anzhong Building, Campus Zijingang, Zhejiang University, No.388 Yuhangtang Road, Hangzhou, China. **E-mail:** chiangym@zju.edu.cn

Qihua Ran:

Postal address: Room B519, Anzhong Building, Campus Zijingang, Zhejiang University, No.388 Yuhangtang Road, Hangzhou, China. **E-mail:** ranqihua@zju.edu.cn

Yue-Ping Xu:

Postal address: Room B513, Anzhong Building, Campus Zijingang, Zhejiang University, No.388 Yuhangtang Road, Hangzhou, China. **E-mail:** yuepingxu@zju.edu.cn

2. Corresponding author:

Yue-Ping Xu

Tel.:+86 15924171902. *E-mail address:* yuepingxu@zju.edu.cn (Y-P Xu).

Postal address: Room B513, Anzhong Building, Campus Zijingang, Zhejiang University, No.388 Yuhangtang Road, Hangzhou, China.

The research was conducted at Zhejiang University.

A two-step sensitivity analysis for hydrological signatures in Jinhua River Basin, East China

Suli Pan^a, Guangtao Fu^b, Yen-Ming Chiang^a, Qihua Ran^a and Yue-Ping Xu^{a,*}

^a Institute of Hydrology and Water Resources, College of Civil Engineering and Architecture, Zhejiang University, Hangzhou, 310058, China

^b Center for Water Systems, College of Engineering, Mathematics and Physical Sciences, University of Exeter, North Park Road, Harrison Building, Exeter, EX4 4QF, UK

Abstract

Parameter calibration and sensitivity analysis are usually not straightforward tasks for distributed hydrological models, owing to the complexity of model and large number of parameters. A two-step sensitivity analysis approach is proposed for analyzing the hydrological signatures based on the Distributed Hydrology-Soil-Vegetation Model in Jinhua River Basin, East China. A preliminary sensitivity analysis is conducted to obtain influential parameters via Analysis of Variance. These parameters are further analyzed through a variance-based global sensitivity analysis method to achieve robust rankings and parameter contributions. Parallel computing is designed to reduce computational burden. The results reveal that only a few parameters are significantly sensitive and the interactions between parameters could not be ignored. When analyzing hydrological signatures, it is found that water yield was simulated very well for most samples. Small and medium floods are simulated very well while slight underestimations happen to large floods.

* Corresponding author at: Institute of Hydrology and Water Resource, College of Civil Engineering and Architecture, Zhejiang University, room B513, Anzhong Building, No.388 Yuhangtang Road, Hangzhou 310058, China.

Tel.: +86 15924171902. E-mail address: yuepingxu@zju.edu.cn (Y-P Xu).

63 **Key words:** Sensitivity analysis, ANOVA method, Sobol's method, Hydrological signature,
64 DHSVM, Peak flow

65 **1 Introduction**

66 Distributed physically-based hydrological models have obtained ever-growing attention in
67 recent decades owing to consideration of spatial variability and widely applications for ungauged
68 basins (Razavi and Coulibaly 2012, Zhan *et al.* 2013, Palanisamy and Workman 2014, Noori *et al.*
69 2014, Noori and Kalin 2016). Applications of these models are wide, including impact analysis of
70 climate change and land cover, runoff and flood forecasting, and improving insights of
71 hydrological process (Du *et al.* 2012, Rahman *et al.* 2013, Xu *et al.* 2013, Tan *et al.* 2015,
72 Winchell *et al.* 2015, Cao *et al.* 2016, Chen *et al.* 2016).

73 However, the applications of distributed hydrological models for these fields depend on the
74 performance of model simulation, which is optimized by model calibration (Bittelli *et al.* 2010,
75 Cibin *et al.* 2010). Hydrological models are characterized by a set of parameters, varying from
76 simple lumped rainfall-runoff models with several parameters to sophisticated, distributed models
77 with large numbers of parameters, even hundreds (Moradkhani and Sorooshian 2008). Therefore,
78 manual calibration for distributed hydrological models with all parameters is time consuming and
79 practically difficult to find optimal parameter sets. Likewise, a lack of identification for influential
80 parameters in model simulation may cause waste of time on un-influential parameters (Bahreman
81 and De Smedt 2008). Hence, it is very essential to identify the dominant parameters controlling
82 model behavior, which contributes to raising calibration efficiency and obtaining more satisfactory
83 simulation. One useful approach of dominant parameter identification is through implementation

1
2
3
4 84 of sensitivity analysis (SA), which can quantify the influence of parameters on model response
5
6 85 (Wagener *et al.* 2001, Xu and Mynett 2006, Tang *et al.* 2007b, Zhang *et al.* 2013, Zhan *et al.* 2013,
7
8 86 Song *et al.* 2015, Ren *et al.* 2016). The results of sensitivity analysis are helpful to determine
9
10
11 87 sensitive parameters which should be paid more attention to in model calibration. A
12
13 88 comprehensive comparison of various sensitivity analysis methods are implemented in literatures
14
15 89 (Saltelli *et al.* 2000b, Saltelli *et al.* 2004, Tang *et al.* 2007b) and the results reveal that the Sobol's
16
17 90 method is the effective method to obtain global parameter sensitivities. Furthermore, Tang *et al.*
18
19 91 (2007a) applied the Sobol's method to a distributed hydrological model and obtained robust
20
21 92 sensitivity rankings of the parameters, which could be able to significantly reduce the number of
22
23 93 parameters for calibrating a hydrological model.
24
25
26

27
28 94 Hydrological signatures are often used to quantify hydrological input variables and response
29
30 95 variables (Yadav *et al.* 2007, Westerberg and McMillan 2015). Signatures are widely used for
31
32 96 catchment classification (Wagener *et al.* 2007, Sawicz *et al.* 2011), change detection (Archer and
33
34 97 Newson 2002) and model calibration (Gupta *et al.* 2008). Yadav *et al.* (2007) adopted hydrological
35
36 98 signatures (slope of the flow duration curve (FDC) and runoff ratio) and similarity indices for
37
38 99 catchments classification. Hartmann *et al.* (2013a, 2013b) evaluated hydrological model
39
40 100 performance with respect to hydrological signatures. Likewise, Westerberg *et al.* (2011) applied
41
42 101 several points selected on FDC for model calibration and two selection methods are compared to
43
44 102 estimate their impacts on parameter calibration. Furthermore, the application of hydrological
45
46 103 signatures in hydrological modeling can offer meaningful information contained in hydrographs.
47
48 104 Signatures could also help to interpret the relations between models and underlying hydrological
49
50 105 processes and reflect various aspects of model behaviors.
51
52
53
54
55
56
57
58
59
60

1
2
3
4 106 The Distributed Hydrology-Soil-Vegetation Model (DHSVM) (Wigmosta *et al.* 1994), a fully
5
6 107 distributed hydrological model, is characterized by numerous parameters. It does not contain any
7
8 108 sensitivity analysis or model calibration module. Therefore sensitivity analyses for DHSVM are
9
10
11 109 often implemented using one-factor-at-a-time (OFAT) (Cuo *et al.* 2011), a local sensitivity test
12
13 110 using stepwise, single parameter perturbation method (Du *et al.* 2014) and method of Morris
14
15 111 (Kelleher *et al.* 2015). These SA methods are all simple or local and could not fully represent the
16
17 112 relations between input parameters and model outputs due to their few sample sizes for lots of
18
19 113 parameters and the interactions among parameters are often ignored. In this study, a two-step
20
21 114 approach is therefore proposed for in-depth sensitivity analysis for DHSVM by adding two SA
22
23 115 modules (Sobol's and Analysis of Variance (ANOVA) methods, and iterated fractional factorial
24
25 116 design (IFFD) sampling approach is applied in ANOVA to reduce the computational burden) into
26
27 117 the DHSVM model, which can provide robust sensitivity rankings and parameter's individual
28
29 118 contributions, total contributions and interactions. Additionally, the parameters values for different
30
31 119 soil and vegetation types are distinct in this study. In order to fully evaluate the performance of
32
33 120 DHSVM, several hydrological signatures are selected in this study.
34
35
36
37
38
39

40 121 The structure of this paper is as follows. Section 2 describes the material and methods used in
41
42 122 the study. Section 3 presents the results of two-step sensitivity analysis and analysis of
43
44 123 hydrological signatures. Section 4 provides discussion concerning the two-step sensitivity analysis
45
46 124 approaches and its further application in future. Section 5 summarizes the findings in this study.
47
48
49
50
51
52
53
54
55
56
57
58
59
60

1
2
3
4 125 **2 Material and methods**

5
6
7
8 126 *2.1 Methodology framework*

9
10
11 127 The methodology framework of this study is presented in Figure 1. The first step is to
12
13 128 prepare input data for the hydrological model and determine ranges of nearly all parameters.
14
15 129 ANOVA sensitivity analysis is then undertaken to obtain preliminary sensitive parameters in the
16
17 130 first step. This is because that model outputs are assumed to be normally distributed. Substantial
18
19 131 departures from the assumption of normality can affect sensitivity analysis results (Lindman,
20
21 132 1974) and the results of ANOVA sensitivity analysis may not be robust. Therefore, only the
22
23 133 effect of individual parameters is adopted in the study. Additionally, the number of model runs in
24
25 134 ANOVA method is smaller than that in the Sobol's method used in the second step. These
26
27 135 preliminary sensitive parameters from ANOVA are further analyzed via Sobol's method to
28
29 136 achieve robust results, including effects of individual parameters and interactions between
30
31 137 parameters. Afterwards, final sensitive parameters and their interactions are quantified and
32
33 138 ranked. The third step is to interpret the impact of final sensitive parameters on model simulation
34
35 139 through considering objective functions, sensitivity index and values of parameters. The fourth
36
37 140 step is to execute hydrological signature analysis and percentile analysis for peak flows for
38
39 141 samples with efficiency criteria > 0.7 . Moreover, detailed signatures analysis and percentile
40
41 142 analysis are done for selected individual samples.
42
43
44
45
46
47
48

49
50 143 **Figure 1.** Methodology framework used in this study.
51
52
53
54
55
56
57
58
59
60

144 2.2 Study area

145 Jinhua River, a tributary of Qiantang River, is located in the Midwest of Zhejiang Province,
146 East China (Figure 2). This river has a length of 195 km and the catchment area is 6 782 km² (Xu
147 *et al.* 2015). In this study, the basin above Jinhua hydrological station is included and its
148 catchment area is 5 996 km², which is appropriate to apply DHSVM model (the model is mainly
149 applicable to watersheds whose area is less than 10 000 km²). Also this model has been
150 successfully used in the study area (Xu *et al.* 2015). The prevailing climate of the basin is Asian
151 subtropical monsoon, which is characterized by abundant precipitation and high temperature in
152 summer and rainless and cold winter. The annual average temperature is 17 °C. The elevation
153 ranges from 29 to 1 296 m in the basin (Figure 3). The annual mean precipitation is 1 424 mm.
154 More than 50% of the annual total precipitation happens in the period from May to July. Because
155 of the unevenly temporal distribution of precipitation, Jinhua River Basin suffers a lot from
156 droughts and floods. Good hydrological simulation will provide support to disaster prediction
157 and prevention, and sustainable river management. Figure 2 also presents the locations of five
158 meteorological stations and the hydrological station used in the study.

159 **Figure 2.** Location of the six stations used in the study.

160 2.3 Overview of DHSVM

161 Distributed Hydrology-Soil-Vegetation Model (DHSVM) (Wigmosta *et al.* 1994, Wigmosta
162 and Burges 1997, Wigmosta *et al.* 2002) is a physically-based distributed hydrological model.
163 DHSVM provides an integrated representation of hydrology-vegetation dynamics at the spatial
164 scale identified by digital elevation map (DEM) data (the spatial resolution is typically 10-200

1
2
3
4 165 m). The river basin is separated into computational grid cells depending on DEM. Soil and
5
6 166 vegetation characteristics are allocated to each computational grid cell. At each time step,
7
8 167 DHSVM offers simultaneous solution to water and energy balance equations for every grid cell
9
10
11 168 in the river basin. The hydrological connection of individual grid cell is realized by surface and
12
13 169 subsurface flow routing. The spatial and temporal resolutions are 200 m and daily respectively.
14
15
16 170 The version 3.1.1 of DHSVM is adopted in this study.

17
18 171 DHSVM consists of seven modules, i.e., evapotranspiration, snowpack accumulation and
19
20 172 melt, canopy snow interception and release, unsaturated moisture movement, saturated
21
22 173 subsurface flow, surface overland flow and channel flow (Wigmosta *et al.* 2002).
23
24
25 174 Evapotranspiration is presented adopting a two-layer canopy model with both two layers divided
26
27 175 into wet and dry areas. Modules concerning snow, i.e., snowpack accumulation and melt and
28
29 176 canopy snow interception and release, are not considered here owing to the fact that snow is rare
30
31 177 in the study area. Unsaturated moisture movement with multiple root zone soil layers is assessed
32
33 178 utilizing Darcy's Law (Domenico and Schwartz 1988). Every grid cell exchanges available water
34
35 179 with its adjacent grid cells using a function of its hydraulic conditions bringing about a transient,
36
37 180 three-dimensional formulation of saturated subsurface flow and surface flow. DHSVM adopts a
38
39 181 cell-by-cell method to route saturated subsurface flow utilizing a kinematic or diffusion
40
41 182 approximation (Wigmosta *et al.* 1994, Wigmosta and Lettenmaier 1999). Grid cells in the basin
42
43 183 are centered on each DEM point.
44
45
46
47
48
49

50 184 Surface runoff is routed by a unit hydrograph method or an explicit cell-by-cell method (the
51
52 185 explicit cell-by-cell approach is adopted in this study). Surface runoff occurs in a cell when
53
54 186 meeting any of the following conditions: firstly, the available water in grid cell exceeds the
55
56
57
58
59
60

1
2
3
4 187 defined infiltration capacity; secondly, the water table exceeds the ground surface. The
5
6 188 downslope movement of surface runoff is based on a cell-by-cell mode which is similar to the
7
8 189 approach applied for subsurface flow. Flow in stream channels and road drainage ditches is
9
10 190 routed by utilizing a cascade of linear channel reservoirs. Roads are not considered in this study
11
12 191 owing to the fact that detailed road information is not available and the area percentage of roads
13
14 192 is very small compared to the big basin area. However, it is kept in the mind that roads often
15
16 193 generate overland flow from compacted surfaces, intercept subsurface flow at road cuts and alter
17
18 194 hillslope hydrologic processes. Ignoring the roads may affect the accuracy of hydrological
19
20 195 simulation, in particular peak and peak time. In the model, lateral inflow to a channel segment,
21
22 196 from the cells which it passes through, is composed of subsurface flow and overland flow
23
24 197 intercepted by channels.

25
26
27
28
29
30 198 Generally, DHSVM parameters can be classified into elevation, stream, road, soil and
31
32 199 vegetation categories. Parameters related to the characteristics of stream network such as stream
33
34 200 segment length, width and aspect are determined based on the DEM data. That is to say, these
35
36 201 parameters do not need to be calibrated. Soil/vegetation parameters such as field capacity need to
37
38 202 be calibrated if its real value in physical meaning is not known or no observation is available.
39
40 203 The calibration of vegetation and soil parameters in DHSVM is very common in other studies
41
42 204 (Thanapakpawin *et al.* 2007, Safeeq and Fares 2012, Cuartas *et al.* 2012).

43 205 *2.4 Model input data*

44
45
46
47
48
49
50
51 206 The climate data including average air temperature, wind speed, relative humidity, sunshine
52
53 207 duration and precipitation from five meteorological stations, i.e., Jinhua, Dongyang, Wuyi,

1
2
3
4 208 Yongkang and Yiwu (Figure 2), are available in this study. The climate data is obtained from
5
6 209 Zhejiang Provincial Metrological Administration. The incoming shortwave radiation and
7
8 210 longwave radiation are calculated using climate data. The observed runoff at Jinhua hydrological
9
10 211 station is obtained from Zhejiang Provincial Hydrology Bureau (Figure 2). The time period of
11
12 212 climate and runoff data is from 1991-2000.

13
14
15 213 The other data needed for DHSVM include watershed boundary (mask), digital elevation
16
17 214 map (DEM), soil type, vegetation type, soil depth and streams network. The DEM data (Figure 3)
18
19 215 with a resolution of 90 m are downloaded from the Shuttle Radar Topography Mission (SRTM)
20
21 216 website (<http://srtm.csi.cgiar.org/>). Considering computational burden, the resolution of DEM is
22
23 217 redefined to 200 m in the model. The water boundary is determined based on DEM. The soil data
24
25 218 (Figure 3) are obtained from Nanjing Institute of Soil Research, China. According to the USDA
26
27 219 (United States Department of Agriculture) soil texture classification system needed in DHSVM,
28
29 220 the soil classes are reclassified. The vegetation data (Figure 3) are obtained from WESTDC Land
30
31 221 Cover Products 2.0 (2006) (<http://westdc.westgis.ac.cn>). Table 1 shows vegetation and soil
32
33 222 classes and their percentages in Jinhua River Basin. The soil depth and streams network are
34
35 223 generated based on DEM and mask using Arc Workstation.

36
37
38 224 **Figure 3.** DEM (digital elevation map) (a) soil distribution (b) and vegetation distribution (c) in Jinhua River Basin.

39
40
41 225 **Table 1.** Vegetation and soil classes and their percentages in Jinhua River Basin.

42 43 44 45 46 47 48 226 *2.5 Analysis of Variance (ANOVA) sensitivity analysis*

49
50
51 227 For this study, Analysis of Variance (ANOVA) is adopted to determine the preliminary
52
53 228 sensitive parameters in DHSVM simulation owing to its popularity and common application (Steel

1
2
3 and Torrie 1988, Shinohara *et al.* 2016). In this method, parameters are sorted into specific scope of
4
5
6 230 parameter values indicating intervals with same parameter value width. Based on ANOVA
7
8 231 terminology, inputs are referred to as “factor” and values of factors are referred to as factor levels.
9
10
11 232 Moreover, output is called “response variable”. ANOVA method was proposed by Fisher (1925).
12
13 233 The F value is a key statistic in ANOVA and describes the statistical significance of differences in
14
15
16 234 the mean responses among the levels of corresponding parameter. Therefore, the F values are
17
18 235 utilized to judge whether parameter causes difference in response variable, i.e. sensitivity. The
19
20
21 236 higher the F value is, the more crucial parameter is. Then, the parameter is more sensitive in
22
23 237 model simulation. The equation of F value is described as follows:

24
25
26 238
$$F = \frac{\bar{S}_A}{\bar{S}_E} \quad (1)$$

27
28

29 239 Where \bar{S}_A is referred to group (treatment) mean squares from factor A , which reflects the
30
31 240 differences between mean value of samples in different levels and mean value of all samples. \bar{S}_E
32
33
34 241 is referred to error (residual) mean squares, which reflects the differences between value of each
35
36
37 242 sample and mean value of samples in different levels.

38
39 243 One-way ANOVA is used to evaluate the significance of one factor on response variable.
40
41 244 Two-way ANOVA is dealt with two or multiple factors and applied to determine the single effect
42
43
44 245 of factor and interaction effects between factors. No assumption is demanded regarding the
45
46
47 246 functional form of relationships between the outputs and the inputs in ANOVA. Generally,
48
49 247 ANOVA method could apportion the variance, but substantial departures from the assumption of
50
51 248 normality can affect analysis results (Lindman, 1974). Therefore, only the effect of individual
52
53
54 249 parameter is adopted in the study.

55
56 250 ANOVA will become computationally infeasible if the number of input is large. The number

1
2
3
4 251 of model runs could be decreased and computational efficiency will be much higher by using
5
6 252 IFFD sampling approach (Saltelli *et al.* 1995, Andres 1997). In IFFD, parameters are sampled at
7
8 253 three different levels (groups): low, middle and high, rather than from a continuous range (Saltelli
9
10 254 *et al.* 1995). These discrete levels are defined equally within the original parameter scope. The use
11
12
13 255 of a slight number of factor levels empowers the sampling formula to achieve results effectively
14
15 256 and accurately (Andres 1997). In Jinhua River Basin, there are ten vegetation classes and six soil
16
17 257 classes. The number of parameters is more than 200, if all soil and vegetation classes are included.
18
19
20 258 Because there is hardly any snow in the study area, parameters concerning snow are excluded in
21
22 259 sensitivity analysis. Moreover, soil and vegetation classes are only chosen when their area
23
24 260 percentages in the basin are higher than 10%. Thus, the vegetation and soil classes in italic script
25
26 261 in Table 1 are selected. In total, three soil classes, i.e., sandy loam (SL), loam (L) and clay loam
27
28 262 (CL), and three vegetation classes, i.e., mixed forests (MF), grasslands (GL) and cropland (CrL)
29
30 263 are finally considered in ANOVA sensitivity analysis. The total percentages for selected soil and
31
32 264 vegetation classes are about 90%. Consequently, in ANOVA sensitivity test, the number of
33
34 265 parameters is 83 and the sample size is 14 000. According to Cuo *et al.* (2011), model simulation
35
36 266 is sensitive to both vegetation height and vegetation minimum resistance. Different parameter
37
38 267 ranges are used for these vegetation parameters in different vegetation stories (as shown in Table 2,
39
40 268 italic). Ranges, unit and abbreviation of selected parameters are presented in Table 2. Besides,
41
42 269 monthly LAI in different months is distinguished via appropriate multipliers and the ranges of LAI
43
44 270 in Table 2 are represented for January which has the minimum LAI.
45
46
47
48
49
50
51

52 **Table 2.** Ranges, unit and abbreviation of constant, soil and vegetation parameters for ANOVA sensitivity analysis.
53
54
55
56
57
58
59
60

272 *2.6 Sobol's sensitivity analysis*

273 Sobol's sensitivity analysis method (Saltelli *et al.* 2000a, Sobol' 2001), a variance-based
 274 method, is selected in this study for in-depth global sensitivity analysis since this method is able
 275 to quantify not only the contributions of individual parameter to DHSVM simulation but also
 276 their interactions, which could not be obtained accurately from ANOVA (Zhang *et al.* 2013, Xu
 277 *et al.* 2014). In addition, sensitivity index provided by the Sobol's method are more effective
 278 than other sensitivity analysis methods for its capability of describing the interactions between a
 279 large number of variables for extremely nonlinear models, such as distributed hydrological
 280 models (Tang *et al.* 2007a, Tang *et al.* 2007b, Rajabi *et al.* 2015). In this method, the attribution
 281 of total output variance to individual model parameters and their interactions can be defined as
 282 follows (Bois *et al.* 2008):

$$283 \quad V = \sum_i (V_i) + \sum_{i < j} (V_{ij}) + \sum_{i < j < m} (V_{ijm}) + \dots + (V_{1,2,\dots,k}) \quad (2)$$

284 Where V is the total variance of model output; V_i is the first order variance for the i th
 285 variable x_i ; V_{ij} is the interaction variance between x_i and x_j ; k is the total number of input
 286 variables. The variances displayed in Equation (2) can be assessed by approximate Monte Carlo
 287 numerical integrations. The sensitivity of individual parameters or their interactions,
 288 i.e. sensitivity index are calculated according to their contribution in the total variance V .

$$289 \quad \text{First order sensitivity index } S_i = \frac{V_i}{V} \quad (3)$$

$$290 \quad \text{Second order sensitivity index } S_{ij} = \frac{V_{ij}}{V} \quad (4)$$

$$291 \quad \text{Total order sensitivity index } S_{Ti} = \frac{\sum_i (V_i) + \sum_{i < j} (V_{ij}) + \sum_{i < j < m} (V_{ijm}) + \dots + (V_{1,2,\dots,k})}{V} \quad (5)$$

292 Where S_i is the first order sensitivity index corresponding to the input factor x_i ; the second

293 order sensitivity index S_{ij} evaluates the interactions between x_i and x_j ; the total order sensitivity
 294 index S_{Ti} calculates the total effects of the input factor x_i on the model simulation.

295 2.7 Objective function and parallel computing

296 The proper choice of an objective function is often demanded for evaluating the performance
 297 of a hydrological model in sensitivity analyses and model calibration, but not essential (Hartmann
 298 *et al.* 2015, Pianosi *et al.* 2016). Objective function must be able to accurately express the distance
 299 between observation and simulation. Comprehensive objective functions and efficiency criteria
 300 have been used in hydrological simulation (Rao and Han 1987, Yan and Haan 1991). In the study,
 301 Nash-Sutcliffe efficiency (NS) is firstly selected. NS is a normalized statistic that confirms the
 302 relative difference of residual variance in contrast to observation variance (Nash and Sutcliffe,
 303 1970). NS is calculated as shown in Equation (6). NS is more sensitive to peak flows than low
 304 flows because squared deviations is utilized which leads to the possibility that low flows is not
 305 accurately simulated by hydrological models (Schaefli and Gupta 2007, Criss and Winston 2008,
 306 Muleta 2012, Hartmann *et al.* 2015). E_{rel} (Equation (7)) is a statistic which is widely applied to
 307 evaluate the performance of low flow simulation (Krause *et al.* 2005, Raposo *et al.* 2012). The
 308 combination with equal weights (NE ; Equation (8)) is then used as the final objective function in
 309 this study. The relevant equations are shown as follows:

$$310 \quad NS = 1 - \frac{\sum_{i=1}^n (O_i - S_i)^2}{\sum_{i=1}^n (O_i - \bar{O})^2} \quad (6)$$

$$311 \quad E_{rel} = 1 - \frac{\sum_{i=1}^n \left(\frac{O_i - S_i}{O_i} \right)^2}{\sum_{i=1}^n \left(\frac{O_i - \bar{O}}{\bar{O}} \right)^2} \quad (7)$$

$$312 \quad NE = 0.5 \times NS + 0.5 \times E_{rel} \quad (8)$$

1
2
3
4 314 Where O_i is referred as the observed streamflow; S_i is referred as the simulated streamflow; \bar{O}
5
6 315 is referred as the average of observed streamflow.
7

8 316 DHSVM runs relatively slowly. The meteorological data used in this study are from 1991 to
9
10 317 2000 at daily scale data. The cell grid is 200m and the basin area is 5 996 km². Therefore, each run
11
12 318 of model will take about 50 minutes under Linux server. The run time of DHSVM is 486 days in
13
14 319 ANOVA sensitivity analysis with a sample size of 14 000. Similarly, the run time is 708 days in
15
16 320 Sobol's sensitivity analysis with a set of 20 400 samples. Computer cluster consisting of five PCs
17
18 321 with same configurations is used in this study and the logistical setup of computer cluster is a
19
20 322 master-slave distribution. In other words, one PC plays as master and assigns tasks to slaves, i.e.,
21
22 323 the other four PCs. The slaves receive and finish the tasks from the master. Moreover, in order to
23
24 324 decrease the run interval, the master also participates in running task as well as slaves. And the
25
26 325 configuration in PC is single-CPU (central processing unit) with four cores. Moreover,
27
28 326 Hyper-Threading (with Hyper-Threading, one physical core appears as two processors to the
29
30 327 operating system) is installed in five PCs and the number of processors is then forty. The softwares
31
32 328 which are necessary to be set up in five PCs include gcc, g++, NFS (File Share System), SSH
33
34 329 (Secure Shell) and MPI (Message Passing Interface). The parallel pattern in this study is
35
36 330 data-parallel. That is to say, the tasks for slaves and master are running model based on the sample
37
38 331 sets generated by sensitivity analysis methods, and the process of generating sample sets is done
39
40 332 on the master. The run intervals of ANOVA and Sobol's sensitivity analyses are 13 days and 18
41
42 333 days respectively via parallel computing. The computational efficiency has been greatly enhanced
43
44 334 after parallel computing.
45
46
47
48
49
50
51
52
53
54
55
56
57
58
59
60

1
2
3 335 2.8 Hydrological signatures
4
5

6 336 Hydrological signatures are able to investigate the simulation effect of hydrological models
7
8
9 337 more comprehensively and thoroughly (Yadav *et al.* 2007, Yilmaz *et al.* 2008, Winsemius *et al.*
10
11 338 2009). To analyze the performance of different aspects of streamflow simulated via DHSVM,
12
13
14 339 five distinct conditions of hydrological signatures are selected, including average flow conditions,
15
16 340 low flow conditions, peak flow conditions, duration of flow events for low flow conditions and
17
18
19 341 duration of flow events for peak flow conditions (Olden and Poff 2003, Bormann *et al.* 2011,
20
21 342 Westerberg and McMillan 2015, Shafii and Tolson 2015). The specific hydrological signatures of
22
23
24 343 different conditions are described in Table 3, i.e., mean annual runoff for average flow conditions,
25
26 344 low flow signature and base-flow signature for low flow conditions, specific mean annual
27
28
29 345 maximum flows for peak flow conditions, annual minimum of 1-/3-/7-/30-d means of daily
30
31 346 runoff and annual maximum of 1-/3-/7-/30-d means of daily runoff for duration of flow events.
32
33
34 347 The detailed abbreviation, unit and definition are shown in Table 3.
35

36 348 **Table 3.** Description of the six hydrological signatures used in the study.
37

38 349 In order to evaluate the performance of simulation results conveniently, a new criterion (P)
39
40
41 350 is used and can be calculated by Equation (9). The value of hydrological signatures for observed
42
43
44 351 streamflow is constant. However, P -value of simulated streamflow changes depends on each
45
46 352 parameter set.
47

48 353
$$P = \frac{HS(Q_{sim})}{HS(Q_{obs})} - 1 \quad (9)$$

49

50 354 Where $HS(Q_{obs})$ is referred as the value of hydrological signature for observed streamflow;

51
52
53 355 $HS(Q_{sim})$ is referred as the value of hydrological signature for simulated streamflow.
54

55 356 As shown in Equation (9), if $P > 0$, the value of hydrological signature for simulated
56
57
58
59
60

1
2
3
4 357 streamflow is higher than that of observed streamflow, indicating that the simulated signature is
5
6 358 overestimated. On the contrary, the simulated signature is underestimated. The lower the absolute
7
8 359 value of P is, the higher performance of hydrological model is.

10
11 360 As described in Section 2.1, Jinhua River Basin suffers a lot from floods. Besides the
12
13 361 peak-related hydrological signature shown in Table 3, peak flows extracted from observed and
14
15 362 simulated runoff are compared via percentiles. Here, Peak-over-threshold (POT) (O'Brien *et al.*
16
17 363 2015, Hirsch and Archfield 2015, Mallakpour and Villarini 2015) is adopted to select peak flows.
18
19 364 For POT method, the choice of the threshold is important. If the threshold is too low, excessive
20
21 365 number of peak flows is selected. On contrary, only a few peak flows are considered when the
22
23 366 threshold is too high. In this study, mean of observed daily runoff (1991-2000) is used. Two
24
25 367 subsequent peak events (P_1 and P_2) are identified as independent when the following two
26
27 368 conditions are satisfied (Lang *et al.* 1999):

$$369 \quad \begin{cases} \theta > 5 + \log(Area) \\ X_{\min} < \left(\frac{3}{4}\right) \min(P_1, P_2) \end{cases} \quad (10)$$

36
37 370 Where θ is the interval of two subsequent peak events (days); $Area$ is the area of
38
39 371 watershed (miles²); X_{\min} is the minimum runoff during interval of two subsequent peak events
40
41 372 (m³/s).

42
43 373 Based on these independent conditions and selected threshold, peak flows are extracted
44
45 374 from the observed and simulated runoff in the study period (1991-2000).
46
47
48
49
50
51
52
53
54
55
56
57
58
59
60

375 **3 Results**

376 *3.1 ANOVA sensitivity analysis result*

377 Figure 4 presents the F -value and percentage of the total variance at a significance level of
378 $p=0.05$. Sixteen sensitive parameters are preliminarily selected from all parameters (83) of
379 DHSVM, based on the criterion that F -Value is bigger than 3.0. The sum of variance percentages
380 of selected sixteen parameters is about 97.6%. The higher the F -value is, the more sensitive the
381 parameter is.

382 Figure 4 shows that F -values of some parameters exceed three orders of magnitude larger
383 than 3.0. Hence, a threshold of 300 is adopted to determine whether a parameter is highly
384 sensitive or not. There are three highly sensitive parameters, i.e., rain LAI multiplier (R_j),
385 porosity of clay loam ($\phi(CL)$) and field capacity of clay loam ($\theta_{fc}(CL)$), accounting for 19.3%,
386 9.6% and 40% of total variance respectively. Among these highly sensitive parameters, field
387 capacity of clay loam is the most sensitive parameter and its F -value is 1 583.4 which is far
388 larger than the threshold 300. Field capacity together with root zone depth ($D(CrL)$) determines
389 realistic storage of available water in soil, and realistic storage will diminish with the decrease of
390 field capacity. Consequently, the same amount water access soil subsurface layers will have
391 higher runoff with decreasing field capacity. However, porosity together with root zone depth
392 decides the capacity of water in soil. Simulated peak flows will decrease and routing time will
393 increase with increasing porosity. Rain LAI multiplier is LAI multiplier for rain interception,
394 which will influence interception storage and evaporation.

395 Thirteen sensitive parameters are presented in Figure 4, including five soil parameters

1
2
3
4 396 (mainly from clay loam) and eight vegetation parameters (related to mixed forests and croplands).
5
6 397 Understory minimum resistance ($UR_{min}(MF)$) and overstory minimum resistance
7
8 398 ($OR_{min}(MF)$) of mixed forest are sensitive parameters. According to Wigmosta *et al.* (2002),
9
10 399 canopy resistance is calculated separately for the understory and overstory. Similarly, understory
11
12 400 height ($Uh(MF)$) of mixed forest is sensitive to simulated streamflow. Additionally, in reality, the
13
14 401 actual values for understory and overstory height of mixed forest are different. Vegetation height
15
16 402 is related to aerodynamic resistance, which determines the rate of potential evaporation with
17
18 403 other parameters. Vegetation minimum resistance, vapor pressure deficit ($Ec(CrL)$) and soil
19
20 404 moisture threshold ($\theta^*(CrL)$) are used to calculate canopy resistance, which directly impact
21
22 405 vegetation transpiration. LAI affects the capacity of canopy interception and acquisition of solar
23
24 406 radiation. Therefore, the rate of potential evaporation will increase with increasing LAI. Lateral
25
26 407 conductivity ($K(CL)$) is used in the calculation of lateral flow movement and lateral conductivity
27
28 408 exponential decrease ($f(CL)$) describes exponent decrease of lateral conductivity with soil depth.
29
30 409 Both of them influence the amount of lateral flow and routing time. Wilting point ($\theta_{wp}(CL)$,
31
32 410 $\theta_{wp}(L)$) and bulk density ($\rho_B(CL)$) are related to soil evaporation.
33
34
35
36
37
38
39
40 411 **Figure 4.** ANOVA parameter sensitivities based on the *NE* measure (F -value > 3).
41

42
43 412 Figure 5 shows the observed and simulated hydrographs (when the value of *NE* is the
44
45 413 maximum in ANOVA sensitivity analysis) of 1994, 1995 and 1996, which correspond to
46
47 414 moderate, wet and dry year respectively. The efficiency criteria for *NS*, E_{rel} and *NE* (1991-2000
48
49 415 years) are 0.83, 0.81 and 0.82 respectively, which show a good performance of the hydrological
50
51 416 model. In addition, the bias is -7.8%, which is well within the range -25%~25% (Safeeq and
52
53 417 Fares 2012, Xu *et al.* 2015). However, the runoff, especially peak flow, is slightly underestimated.
54
55
56
57
58
59
60

1
2
3
4 418 In general, the simulation demonstrates that DHSVM is able to simulate river flows in a good
5
6 419 way. Also it can be observed from Figure 5 that the model performance in the dry year (1996) is
7
8 420 better than that in the moderate year (1994).

9
10 421 **Figure 5.** Model performance in 1994, 1995 and 1996 (corresponding to moderate, wet and dry year, respectively) when the
11
12 422 value of NE (NS , E_{rel} and NE are 0.83, 0.81 and 0.82 respectively) is the maximum in ANOVA sensitivity analysis.

13 14 15 16 423 *3.2 Sobol's sensitivity analysis results*

17
18
19
20 424 The input factors for Sobol's sensitivity test are preliminary sensitive parameters selected by
21
22 425 ANOVA (as shown in Figure 4 and Table 4). As shown in Table 4, sixteen model parameters are
23
24 426 considered in Sobol's sensitivity analysis and a sample size of 20 400 is used (according to
25
26 427 Saltelli and Tarantola (2002), this sample size is appropriate). Saltelli (2000a) extended the
27
28 428 Sobol's original work by adding special transformation to the randomly sampled parameters to
29
30 429 reduce computational complexity. This transformation is used in this study and the ranges of
31
32 430 porosity, field capacity and wilting point of clay loam are slightly changed (Italic in Table 4). The
33
34 431 value of NE ranges from 0.2 to 0.88. Percentage of samples with NE value higher than 0.8, is up
35
36 432 to 66.7%. Percentage of E_{rel} that is larger than 0.8 accounts for nearly 60% and the highest value
37
38 433 of E_{rel} is 0.93. Moreover, a majority of samples has a value of NS higher than 0.7. In addition,
39
40 434 biases are also calculated for all samples, and nearly all values are within the acceptable range of
41
42 435 -25%~25% (Safeeq and Fares 2012). The percentage of correlation coefficient value higher than
43
44 436 0.9 is nearly 97%.

45
46
47
48
49
50
51 437 The total order sensitivity index is shown in Figure 6. Total order sensitivity index of 16
52
53 438 parameters range from 0.00 to 0.29. According to Tang *et al.* (2007b), parameters are highly

1
2
3
4 439 sensitive when the sensitivity indices are higher than 0.1 and sensitive with the indices higher
5
6 440 than 0.01. Parameters are insensitive to streamflow simulation when its total order sensitivity
7
8 441 index is smaller than 0.01. Figure 6 shows that there are eight highly sensitive parameters,
9
10
11 442 including one constant parameter (rain LAI multiplier), four soil parameters (lateral conductivity,
12
13 443 porosity, field capacity and wilting point of clay loam), and three vegetation parameters
14
15 444 (understory monthly LAI, understory minimum resistance and root zone depths of croplands).
16
17
18 445 Compared with the results from ANOVA sensitivity test, it shows that the identified parameters
19
20 446 are similar and the ranking of them is compatible. Moreover, the most sensitive parameter in
21
22
23 447 both methods is field capacity of clay loam. The role of field capacity ($\theta_{fc}(CL)$) is dominant in
24
25 448 unsaturated moisture movement module. In DHSVM model, no unsaturated flow is allowed to
26
27
28 449 occur when the moisture content is below the field capacity. Unsaturated flow will increase with
29
30 450 decrease of field capacity. The amount of runoff is obviously impacted by the value of field
31
32
33 451 capacity. The higher the value of field capacity is, the more runoff will generate. In other words,
34
35 452 more runoff could be obtained by decreasing the value of field capacity. Root zone depth ($D(CrL)$)
36
37
38 453 has significant impacts on unsaturated flow, soil evaporation and the amount of moisture in the
39
40 454 soil column. Model simulation is also highly sensitive to wilting point ($\theta_{wp}(CL)$) and understory
41
42
43 455 LAI ($ULAI(CrL)$), owing to the fact that both of them play important roles in canopy resistance
44
45 456 and evapotranspiration. As shown in Figure 3 and Table 1, the area percentage of forests/mixed
46
47 457 forests is 34.7% (5.0%+0.1%+29.6%), and the area percentage only with understory is 64.5%
48
49
50 458 (1.2%+22.9%+0.4%+36.7%+3.3%). It is easy to overlook that forests/mixed forests also have
51
52
53 459 understory. Additionally, the mixed forest in the study area mainly consists of grasslands,
54
55 460 shrublands and trees. The area percentage of trees in the mixed forest is about 30%, or less.

1
2
3
4 461 Moreover, the vegetation overstory parameters only have slight impacts on canopy interception
5
6 462 and vegetation transpiration. This is an explanation for the conclusion that vegetation parameters
7
8 463 related with overstory are less sensitive to model simulation.
9

10
11 464 **Table 4.** Ranges, number and abbreviation of parameters for Sobol's sensitivity analysis.
12

13
14 465 **Figure 6.** Sobol's total order sensitivity index based on the *NE* measure.
15

16
17 466 Interactions between parameters, i.e., second order sensitivity index, are presented in Figure
18
19 467 7. These interactions could not be identified with other local sensitivity analysis methods, such as
20
21 468 OFAT (One-factor-at-a-time). The x-axis and y-axis are parameter numbers shown in Table 4.
22
23 469 The constant parameter, rain LAI multiplier, has interactions with other fifteen parameters as
24
25 470 shown in the first column of Figure 7. However, all sensitivity indices are smaller than a
26
27 471 threshold value of 0.01, i.e., insensitive interactions. The interactions among field capacity of
28
29 472 clay loam and other parameters are important. The second order sensitivity index between field
30
31 473 capacity of clay loam and understory monthly LAI of croplands is the maximum and the value
32
33 474 reaches 0.03. The total order sensitivity index of field capacity of clay loam reaches 0.29, which
34
35 475 is much larger than its first order sensitivity index (0.18). As presented in Figure 3, clay loam and
36
37 476 croplands covered most areas of the study area. In DHSVM model, LAI has direct effects on
38
39 477 three crucial hydrological processes, i.e., vegetation canopy rainfall interception, evaporation and
40
41 478 soil transpiration. LAI affects acquisition of solar radiation and is used as a multiplier in canopy
42
43 479 precipitation interception. And the rate of potential evaporation will increase with the increase of
44
45 480 LAI and available water into soil will then decrease. Moreover, field capacity is used to
46
47 481 determine the realistic storage of available water in soil. Hence, the streamflow simulation is
48
49 482 proven to be sensitive to the interactions between these parameters.
50
51
52
53
54
55
56
57
58
59
60

1
2
3
4 483 In addition, the interactions between field capacity of clay loam and root zone depth of
5
6 484 croplands are also sensitive, for the reason that field capacity determines plant available water in
7
8 485 soil with root zone depth ($D(CrL)$). The interactions increase the value of total order sensitivity
9
10 486 index of root zone depth to 0.27. Similarly, the interactions between field capacity of clay loam
11
12 487 and soil moisture threshold of croplands are also sensitive. The total sensitivity index of soil
13
14 488 moisture threshold reaches to 0.07, which is much larger than its first order sensitivity index
15
16 489 (0.03). This is due to the fact that soil moisture threshold also has an impact on transpiration of
17
18 490 soil like LAI. Understory height affects evaporation and transpiration of vegetation. This
19
20 491 explains the strong interactions between field capacity and understory height. Likely, the reason
21
22 492 for that model simulation is sensitive to the interactions between field capacity and vapor
23
24 493 pressure deficit is owing to the fact that vapor pressure deficit has an impact on evaporation and
25
26 494 transpiration of vegetation. In addition, vegetation minimum resistance affects water balance and
27
28 495 vegetation transpiration. Both wilting point and LAI have a significant influence on evaporation
29
30 496 of soil. So their interactions are sensitive to model simulation.

31
32
33
34
35
36
37
38 497 **Figure 7.** Interactions among sixteen parameters based on the *NE* measure.

39 40 41 498 *3.3 Hydrological signatures*

42
43
44 499 Six representative hydrological signatures from four flow conditions are selected in this
45
46 500 study. Evaluation criterion *P*-value shown in Equation (9) is used to analyze the performance of
47
48 501 the hydrological model based on hydrological signatures. Figure 8 shows the boxplots of
49
50 502 *P*-values for four hydrological signatures of all samples used in Sobol's sensitivity analysis, i.e.,
51
52 503 mean annual runoff (*AI*), Low flow signature (*LI*), Base-flow signature (*L2*) and Specific mean
53
54
55
56
57
58
59
60

1
2
3
4 504 annual maximum flows (*HI*). For hydrological signature *AI*, *P*-values range from -1.0 to 0.4.
5
6 505 However, the *P*-values between 1% and 99% percentiles are totally within the acceptable scope
7
8 506 (-25%~25%), which illustrates that the overall performance of *AI* is good. For hydrological
9
10 507 signatures *L1*, approximately 96% of *P*-values are bigger than 25%, that is to say, the percentage
11
12 508 for *P*-value within the acceptable range is only 4%. A number of samples are good with the
13
14 509 *P*-value of *L2* close to zero. All of *P*-values of *HI* are lower than zero and 15.8% of *P*-values of
15
16 510 *HI* are within the acceptable scope.

17
18
19
20 511 **Figure 8.** Boxplot for *P*-value of hydrological signatures (*A1* (Mean annual runoff), *L1* (Low flow signature), *L2* (Base-flow
21
22 512 signature): and *H1* (Specific mean annual maximum flows)) of all samples in Sobol's sensitivity analysis.

23
24
25 513 In order to better understand the performance of the model concerning the four hydrological
26
27 514 signatures in some specific samples, four samples with the value of *NE* higher than 0.7 are
28
29 515 selected from all samples in Sobol's sensitivity analysis. Four samples, i.e., *Sample A*, *Sample B*,
30
31 516 *Sample C* and *Sample D*, are selected according to the distinct intervals of *NE* value shown in
32
33 517 Table 5. *Sample A* has the maximum value of *NE*. The results are displayed in Table 6. For
34
35 518 *Sample A*, *P*-value of *AI* is -0.10 and that of *L1*, *L2* and *HI* are 0.68, -0.35 and -0.29 respectively.
36
37 519 This explains that a high value of efficiency criteria could not guarantee good performance in all
38
39 520 aspects of a hydrograph. For *Sample B*, hydrological signature *L1* (0.07) is close to zero and *AI*
40
41 521 (-0.23) also within the acceptable range. *L2* (-0.54) and *HI* (-0.30) indicate less satisfactory
42
43 522 simulations of base flow and peak flow. Nevertheless, base flow is reasonably simulated with *L2*
44
45 523 (0.09) in *Sample C*, so is mean annual runoff (*AI* is equal to 0.01). For *Sample D*, peak flow is
46
47 524 excellently simulated with *HI* (-0.22). Taking the total order sensitivity index (Section 3.2) and
48
49 525 corresponding parameter values in *Sample A* into account, high value of porosity (0.58) and field
50
51
52
53
54
55
56
57
58
59
60

1
2
3
4 526 capacity (0.39) in clay loam result in the inferior performance of hydrological signature *L1*, *L2*
5
6 527 and *H1*.

7
8 528 **Table 5.** Selected samples based on the *NE* value.

9
10
11 529 **Table 6.** Hydrological signatures of the observed and the simulated from selected samples and corresponding *P*-values.

12
13 530 Other hydrological signatures *DH1-4* and *DL1-4* of four selected samples are displayed in
14
15 531 Figure 9 and Figure 10 respectively. For *DH1*, all four samples underestimate annual maximum
16
17 532 of 1-day means of daily runoff in 1991-2000. As shown in Figure 9, the ranking of performance
18
19 533 in *DH1* is *Sample D* > *Sample A* > *Sample B* > *Sample C*. This ranking is similar to that of
20
21 534 hydrological signature *H1*. Underestimation is greatly improved in *DH2*. For *DH3*, four selected
22
23 535 samples perform very well in 1991-2000. For *Sample D*, runoff is mostly overestimated with
24
25 536 minor degrees in all years in *DH4*, which corresponds to hydrological signature *A1* with 0.21 of
26
27 537 *P*-value. Different to *DH1-3*, the ranking of *DH4* is that *Sample C* is the best, *Sample A* is the
28
29 538 second, *Sample B* is the third and *Sample D* is the last. And the ranking of *DH4* is similar to that
30
31 539 based on hydrological signature *A1*.

32
33
34
35
36
37 540 **Figure 9.** Hydrological signature *DH1-4* for observed and simulated runoff from four selected samples as shown in Table 5.

38
39
40 541 As presented in Figure 10, for *DL1*, *Sample B* simulates very well in all years. However,
41
42 542 other three samples underestimate *DL1* during most years. This ranking is totally similar to that
43
44 543 of hydrological signature *L1*. The overestimation is improved for four samples in *DL2*. For *DL3*,
45
46 544 performance of four samples is further better than *DL1* and *DL2*. By comparing the meaning of
47
48 545 *DL3* and *L2*, it is reasonable that the ranking of *DL3* is the same to *L2*. The ranking of *DL4* is
49
50 546 similar to that based on hydrological signature *A1*.

51
52
53
54 547 Hydrological signatures *DH1-4* and *DL1-4* represent maximum and minimum annual flow

1
2
3
4 548 of various durations, which describe the performance of duration of flow event in model
5
6 549 simulation and provide important insights into a hydrograph. As shown in Figure 9 and Figure 10,
7
8 550 the performance of four selected samples in *DHI* and *DLI* is not ideal. However, performance of
9
10 551 *DH3* and *DL3* is good, which illustrates annual maximum and minimum of 7-day means of daily
11
12 552 runoff are reasonably simulated.

13
14
15
16 553 **Figure 10.** Hydrological signature *DLI-4* for observed and simulated runoff for four selected samples as shown in Table 5.

17
18 554 Besides six hydrological signatures described above, peak flow percentile is further used to
19
20 555 explore the performance of peak flow simulation. Figure 11 shows the peak flow percentiles for
21
22 556 the observed and selected samples. These samples are from Sobol's sensitivity analysis samples
23
24 557 and chosen with *NS* higher than 0.7. As presented in Figure 11, Q_{s-1} (1th percentile flows)– Q_{s-70}
25
26 558 (70th percentile flows) are simulated reasonably. However, Figure 11 also shows that extreme
27
28 559 peak flows (with percentile larger than 0.75) are not well simulated which is corresponding to the
29
30 560 performance of hydrological signature *HI* and streamflow curve shown in Figure 5.

31
32
33
34
35 561 **Figure 11.** Peak flow percentiles for observed and simulated runoff from samples whose *NS* > 0.7 in Sobol's sensitivity
36
37 562 analysis.

38
39
40 563 In order to understand the performance of peak flow simulation in individual samples, three
41
42 564 samples are selected based on the *NS* value instead of *NE* value (Considering the fact that the
43
44 565 maximum value of *NS* is 0.85 and *NS* should be bigger than 0.7, three not four distinct intervals
45
46 566 are identified). Three samples, i.e., *Sample PA* (maximum value of *NS*), *Sample PB* and *Sample*
47
48 567 *PC*, are selected according to various intervals of *NS* value shown in Table 7. The results are
49
50 568 shown in Figure 12. For *Sample PA*, Q_{s-1} - Q_{s-25} is simulated very well. However, the other peak
51
52 569 flow percentiles are underestimated in *Sample PA*. The reason for this is the high value of field
53
54
55
56
57
58
59
60

1
2
3
4 570 capacity (0.38) and low value of wilting point (0.07) of clay loam. For *Sample PB*, Q_{s-1} - Q_{s-75}
5
6 571 exhibits slight overestimation. *Sample PC* performs better than the others, Q_{s-1} - Q_{s-70} is totally
7
8 572 consistent to Q_{o-1} - Q_{o-70} and Q_{o-75} - Q_{s-99} shows less underestimation.
9

10
11 573 **Table 7.** Selected samples for peak flow based on the *NS* value.
12

13 574 **Figure 12.** Peak flow percentiles for observed and simulated runoff from three selected samples as shown in Table 7.
14
15

16 17 575 **4 Discussion** 18

19
20
21 576 It is common to apply one sensitivity analysis method to hydrological models and identify
22
23 577 dominant parameters in hydrological model simulation. However, the proposed framework in
24
25 578 this study provides a means to identify parameter sensitivities of DHSVM by using a two-step
26
27 579 sensitivity analysis approach. In the first step, the ANOVA method was used to identify
28
29 580 preliminary sensitive parameters in the DHSVM model simulation. This is because model
30
31 581 outputs are assumed to be normally distributed, which may cause the results of ANOVA
32
33 582 sensitivity analysis not robust. Therefore, only the effect of individual parameters is adopted in
34
35 583 the first step. The ANOVA method was actually used here as a screening sensitivity analysis
36
37 584 method. Then these preliminary sensitive parameters identified by ANOVA were further
38
39 585 analyzed via the Sobol's method to achieve robust results, including effect of individual
40
41 586 parameters and interactions between parameters in the second step. In the end, the performance
42
43 587 of the model was investigated for different parameter sets based on hydrological signatures. As
44
45 588 we explained before, our aim here is to mainly provide parameter identification results for
46
47 589 further calibration and validation. However, we believe during this sensitivity analysis stage,
48
49 590 checking how the different parameter sets play a role in model simulation (through hydrological
50
51
52
53
54
55
56
57
58
59
60

1
2
3
4 591 signature analysis) can also be interesting.
5

6 592 In the two-step sensitivity analysis approach, the Sobol's method can apportion the variance
7
8 593 in model output (streamflow) to the variance in the model parameters and meanwhile consider
9
10 594 interactions among parameters. The results demonstrated that field capacity of clay loam is the
11
12 595 most important, showing the largest total order sensitivity index and high value of interactions
13
14 596 with other parameters. Others sensitive parameters include rain LAI multiplier affecting
15
16 597 evaporation, lateral conductivity and porosity of clay loam contributing to streamflow simulation,
17
18 598 and wilting point of clay loam affecting soil evaporation. Highly sensitive vegetation parameters
19
20 599 consist of understory monthly LAI of croplands influencing evaporation, understory minimum
21
22 600 resistance of croplands strongly affecting water balance and root zone depths of croplands
23
24 601 influencing soil evaporation. These results are in good agreement with that of Du *et al.* (2014)
25
26 602 who showed that vegetation LAI, minimum resistance, porosity, rain LAI multiplier, wilting
27
28 603 point and field capacity are important parameters in the simulation of water yield in northern
29
30 604 Idaho, USA, using a stepwise, single parameter perturbation method. Cuo *et al.* (2011) also
31
32 605 concluded that lateral saturated hydraulic conductivity, porosity, minimum resistance and LAI
33
34 606 should be given special attentions during model calibration based on One-factor-at-a-time
35
36 607 (OFAT). Meanwhile, other literatures have studied parameters sensitivities of DHSVM to model
37
38 608 simulation as well (Surfleet *et al.* 2010, Kelleher *et al.* 2015). Nevertheless, the sensitivity
39
40 609 analysis methods used in these studies could only obtain single contribution of parameters or less
41
42 610 robust sensitivity results. The Sobol's method is able to achieve robust sensitivity rankings and,
43
44 611 what's more, the interactions between parameters. In particular, in the current study, the
45
46 612 interactions between field capacity of clay loam and other parameters cannot be ignored. As
47
48
49
50
51
52
53
54
55
56
57
58
59
60

1
2
3
4 613 shown in Figure 6, the total order sensitivity index becomes 0.29, which is much larger than the
5
6 614 first order sensitivity index (0.18) after considering the interactions. This study demonstrates that
7
8 615 the Sobol's method did provide valuable information to parameter selections in DHSVM
9
10 616 calibration, and promote further guides in searching for optimal parameter sets for this model
11
12
13 617 through considering parameter interactions.

14
15
16 618 In this study, several soil and vegetation types whose area percentages are bigger than 10%
17
18 619 were considered in the two-step sensitivity analysis. Simplified soil and vegetation classes in the
19
20 620 sensitivity analysis for DHSVM model may have an impact on simulation results (Cuo *et al.*
21
22
23 621 2011, Surfleet *et al.* 2010, Du *et al.* 2014). For instance, it is obvious that model simulation will
24
25 622 be affected if same values were set for overstory vegetation LAI of evergreen needleleaf forests
26
27
28 623 and evergreen broadleaf forests. Likewise, it is unrealistic that same values were set for field
29
30 624 capacity of clay and sand.

31
32
33 625 It should be noted that four hydrological signatures could not be well simulated
34
35 626 simultaneously in any individual sample from Sobol's sensitivity analysis. Hence, in order to
36
37
38 627 obtain better model simulation, multi-objective calibration is necessary to achieve optimal
39
40 628 parameter sets. Considering the complexity of model and large number of parameters, manual
41
42
43 629 calibration is inefficient and difficult to obtain global optimal parameter sets. Automatic
44
45 630 calibration is preferred for DHSVM with parallel computing to reduce computational burden.
46
47
48 631 Traditional calibration is usually performed with a single objective (Guo *et al.* 2014, Wang and
49
50 632 Brubaker 2015). However, a single objective is often inadequate to meet multiple requirements
51
52
53 633 (Vrugt *et al.* 2003). Efficient global optimization algorithms are therefore recommended for use
54
55 634 to reliably search for the global optimal parameter sets (Zhang *et al.* 2013, Ye *et al.* 2014).
56
57
58
59
60

1
2
3
4 635 Peak flow is slightly underestimated in the model simulation of DHSVM. The possible
5
6 636 reasons for this are from various dimensions. Firstly, model structural problems related to peak
7
8 637 flow generation mechanism may exist in DHSVM, including that preferential flow was not
9
10
11 638 considered in this study and the assumption that understory vegetation (if it exist) covers the
12
13 639 entire cell in evapotranspiration mode. Secondly, only limited meteorological stations and daily
14
15 640 scale data are used in the study. According to Booij (2003, 2005), the spatial and temporal
16
17 641 variability of precipitation will affect the hydrological simulation. As shown in the test
18
19 642 application from Wigmosta *et al.* (1994), the best time step of meteorological data for model
20
21 643 simulation is 3-hour. Additionally, determination of appropriate resolution of DEM may be
22
23 644 critical for model simulation. According to Dubin and Lettenmaier (1999), simulations of peak
24
25 645 flow and runoff process are greatly impacted by DEM resolution. Safeeq and Fares (2012) also
26
27 646 concluded that underestimation of the peak flows exist when modeling runoff of a Hawaiian
28
29 647 watershed.
30
31
32
33
34
35
36

37 648 **5. Conclusion**

38
39
40
41 649 In this study, a two-step sensitivity analysis approach was used. Firstly, the sensitivity of
42
43 650 nearly all parameters in DHSVM which was built for Jinhua River Basin, East China, was
44
45 651 roughly analyzed via ANOVA. Sobol's sensitivity analysis method, a variance-based global
46
47 652 sensitivity analysis method, was then applied to analyze the contributions of the preliminary
48
49 653 influential parameters identified by ANOVA to streamflow simulation, including single
50
51 654 contributions, total contributions and interaction contributions. Parallel computing was applied to
52
53 655 reduce the computational burden. For all samples from Sobol's sensitivity analysis, performances
54
55
56
57
58
59
60

1
2
3
4 656 of hydrological signatures were also investigated. Additionally, peak flows extracted from the
5
6 657 observation and simulation via POT approach were compared. The key findings of this study are
7
8 658 summarized below:

9
10
11 659 (1) According to the Sobol's method, only a few number of model parameters are significantly
12
13 660 sensitive in Jinhua River Basin, including a constant parameter (rain LAI multiplier), four
14
15 661 soil parameters (lateral conductivity, porosity, field capacity and wilting point of clay
16
17 662 loam), and three vegetation parameters (understory monthly LAI, understory minimum
18
19
20 663 resistance and root zone depths of croplands). More attention should be paid to these
21
22
23 664 parameters in future model calibration.

24
25 665 (2) The interactions between parameters cannot be ignored. For example, the total order
26
27
28 666 sensitivity index of field capacity of clay loam reaches to 0.29, which is much larger than
29
30 667 the first order sensitivity index (0.18) after considering the interactions between field
31
32
33 668 capacity of clay loam and other parameters.

34
35 669 (3) High value of the objective function (*NE*) didn't indicate excellent performance of
36
37
38 670 hydrological signatures. For most samples from Sobol's sensitivity analysis, water yield
39
40 671 was simulated very well via DHSVM. However, minimum and maximum annual daily
41
42 672 runoffs were underestimated in a majority of samples. And most of seven-day minimum
43
44
45 673 runoffs were overestimated. However, good performances of these three signatures still
46
47
48 674 exist in a number of samples.

49
50 675 (4) The model performances of specific individual samples in percentile analysis were
51
52 676 summarized. Considering sensitive parameters together with their values, the good
53
54
55 677 performance of maximum annual daily runoff in *Sample D* is owing to the low values of
56
57

1
2
3
4 678 rain LAI multiplier, understory monthly LAI and root zone depth. Likewise, *Sample PC*
5
6 679 has the best performance in that its small, medium and large floods show less
7
8 680 underestimation than others.

10 681 (5) Percentiles of peak flows extracted from the observed and simulated runoff indicate that
11
12 682 small and medium floods were simulated reasonably. Slight underestimations happen to
13
14 683 large floods. This is possibly due to the shortcomings of model structure and insufficient
15
16 684 meteorological data used in the study.

18 685 (6) The work in this study helps further multi-objective calibration of DHSVM model and
19
20 686 indicates where to improve to enhance the reliability and credibility of model simulation.
21
22 687 Good simulation of the complete hydrograph is useful for water resources management,
23
24 688 flood prediction and forecasting. Furthermore, the two-step sensitivity analysis approach
25
26 689 can be applied to detailed parameter identification for model simulation with numerous
27
28 690 parameters. The limitation of this approach lies in its demand for a large number of model
29
30 691 runs.

32 692 **Acknowledgements**

33
34
35 693 National Climate Center of China Meteorological Administration, Zhejiang Provincial
36
37 694 Metrological Administration and Zhejiang Provincial Hydrology Bureau are greatly
38
39 695 acknowledged for providing meteorological and hydrological data used in this study. The
40
41 696 valuable comments and suggestions from Editor and three anonymous reviewers are greatly
42
43 697 appreciated.

698 **Funding**

699 This work was supported by National Natural Science Foundation of China (91547106 and
700 51379183), Zhejiang Provincial Natural Science Foundation of China (LR14E090001), and
701 National Key Research and Development Plan "Inter-governmental Cooperation in International
702 Scientific and Technological Innovation"(2016YFE0122100).

704 **Disclosure statement**

705 No potential conflict of interest was reported by the authors.

706 **References**

- 707 Andres, T.H., 1997. Sampling methods and sensitivity analysis for large parameter sets. *Journal of Statistical*
708 *Computation and Simulation*, 57(1-4), 77-110. doi:10.1080/00949659708811804
- 709 Archer, D. and Newson, M., 2002. The use of indices of flow variability in assessing the hydrological and instream
710 habitat impacts of upland afforestation and drainage. *Journal of Hydrology*, 268(1), 244-258.
711 doi:10.1016/S0022-1694(02)00171-3
- 712 Bahremand, A. and De Smedt, F., 2008. Distributed hydrological modeling and sensitivity analysis inTorysa
713 watershed, Slovakia. *Water Resources Management*, 22, 393-408. doi:10.1007/s11269-007-9168-x
- 714 Bittelli, M., et al., 2010. Development and testing of a physically based, three-dimensional model of surface and
715 subsurface hydrology. *Advances in Water Resources*, 33(1), 106-122. doi:10.1016/j.advwatres.2009.10.013
- 716 Bois, B., et al., 2008. Using remotely sensed solar radiation data for reference evapotranspiration estimation at a
717 daily time step. *Agricultural and Forest Meteorology*, 148(4): 619-630. doi:10.1016/j.agrformet.2007.11.005
- 718 Booi, M.J., 2003. Determination and integration of appropriate spatial scales for river basin
719 modelling. *Hydrological Processes*, 17(13), 2581-2598. doi: 10.1002/hyp.1268
- 720 Booi, M.J., 2005. Impact of climate change on river flooding assessed with different spatial model
721 resolutions. *Journal of Hydrology*, 303(1), 176-198. doi: 10.1002/hyp.1268
- 722 Bormann, H., Pinter, N., and Elfert, S., 2011. Hydrological signatures of flood trends on German rivers: Flood
723 frequencies, flood heights and specific stages. *Journal of Hydrology*, 404(1), 50-66.
724 doi:10.1016/j.jhydrol.2011.04.019
- 725 Cao, Q., et al., 2016. Climate and land cover effects on the temperature of Puget sound streams. *Hydrological*
726 *Processes*, 30, 2286-2304. doi: 10.1002/hyp.10784
- 727 Chen, Y., Li, J., and Xu, H., 2016. Improving flood forecasting capability of physically based distributed
728 hydrological models by parameter optimization. *Hydrology and Earth System Sciences*, 20(1), 375-392.
729 doi:10.5194/hessd-12-10603-2015

- 1
2
3 730 Cibin, R., Sudheer, K.P., and Chaubey, I., 2010. Sensitivity and identifiability of stream flow generation
4 731 parameters of the SWAT model. *Hydrological Processes*, 24(9), 1133-1148. doi: 10.1002/hyp.7568
5 732 Criss, R.E. and Winston, W.E., 2008. Do Nash values have value? Discussion and alternate proposals.
6 733 *Hydrological Processes*, 22(14), 2723-2725. doi: 10.1002/hyp
7
8 734 Cuartas, L.A., et al., 2012. Distributed hydrological modeling of a micro-scale rainforest watershed in Amazonia:
9 735 Model evaluation and advances in calibration using the new HAND terrain model. *Journal of Hydrology*,
10 736 462-463, 15-27. doi: <http://dx.doi.org/10.1016/j.jhydrol.2011.12.047>
11 737 Cuo, L., Giambelluca, T.W., and Ziegler, A.D., 2011. Lumped parameter sensitivity analysis of a distributed
12 738 hydrological model within tropical and temperate catchments. *Hydrological Processes*, 25(15), 2405-2421.
13 739 doi: 10.1002/hyp.8017
14
15 740 Domenico, P.A. and Schwartz, F.W., 1998. *Physical and chemical hydrogeology*. New York: Wiley.
16 741 Dubin, A.M. and Lettenmaier, D.P., 1999. Assessing the influence of digital elevation model resolution on
17 742 hydrologic modeling. *University of Washington, Department of Civil and Environmental Engineering: Water*
18 743 *Resources Series*, Technical Report No.159.
19
20 744 Du, E., et al., 2014. Validation and sensitivity test of the distributed hydrology soil-vegetation model (DHSVM) in
21 745 a forested mountain watershed. *Hydrological Processes*, 28(26), 6196-6210. doi: 10.1002/hyp.10110
22 746 Du, J., et al., 2012. Assessing the effects of urbanization on annual runoff and flood events using an integrated
23 747 hydrological modeling system for Qinhuai River basin, China. *Journal of Hydrology*, 464, 127-139.
24 748 doi:10.1016/j.jhydrol.2012.06.057
25
26 749 Fisher, R.A., 1925. *Statistical methods for research workers*. New York: Springer.
27 750 Guo, J., et al., 2014. Multi-objective optimization of empirical hydrological model for streamflow
28 751 prediction. *Journal of Hydrology*, 511, 242-253. doi:10.1016/j.jhydrol.2014.01.047
29 752 Gupta, H.V., Wagener, T., and Liu, Y., 2008. Reconciling theory with observations: elements of a diagnostic
30 753 approach to model evaluation. *Hydrological Processes*, 22(18), 3802-3813. doi: 10.1002/hyp.6989
31 754 Hartmann, A., et al., 2013a. Testing the realism of model structures to identify karst system processes using water
32 755 quality and quantity signatures. *Water Resources Research*, 49, 3345-3358, doi:10.1002/wrcr.20229
33 756 Hartmann, A., 2013b. Process-based karst modelling to relate hydrodynamic and hydrochemical characteristics to
34 757 system properties. *Hydrology and Earth System Sciences*, 17(8), 3305-3321, doi:10.5194/hess-17-3305-2013
35 758 Hartmann, A., et al., 2015. A large-scale simulation model to assess karstic groundwater recharge over Europe
36 759 and the Mediterranean. *Geoscientific Model Development*, 8(6): 1729-1746. doi:10.5194/gmd-8-1729-2015,
37 760 2015.
38 761 Hirsch, R.M. and Archfield, S.A., 2015. Flood trends: not higher but more often. *Nature Climate Change*, 5(3),
39 762 198-199. doi:10.1038/nclimate2551
40 763 Kelleher, C., Wagener, T., and McGlynn, B., 2015. Model-based analysis of the influence of catchment properties
41 764 on hydrologic partitioning across five mountain headwater subcatchments. *Water Resources Research*, 51(6),
42 765 4109-4136. doi: 10.1002/2014WR016147
43 766 Krause, P., Boyle, D.P., and Båse, F., 2005. Comparison of different efficiency criteria for hydrological model
44 767 assessment. *Advances in Geosciences*, 5, 89-97. doi: 1680-7359/adgeo/2005-5-89
45 768 Lang, M., Ouarda, T.B.M.J., and Bobée, B., 1999. Towards operational guidelines for over-threshold
46 769 modeling. *Journal of hydrology*, 225.3: 103-117. doi:[http://dx.doi.org/10.1016/S0022-1694\(99\)00167-5](http://dx.doi.org/10.1016/S0022-1694(99)00167-5)
47 770 Lindman, H.R., 1974. *Analysis of Variance in Complex Experimental Designs*. San Francisco: W. H. Freeman &
48 771 Co.
49 772 Mallakpour, I. and Villarini, G., 2015. The changing nature of flooding across the central United States. *Nature*
50 773 *Climate Change*, 5(3), 250-254. doi:10.1038/nclimate2516
51
52
53
54
55
56
57
58
59
60

- 1
2
3 774 Moradkhani H and Sorooshian S., 2008. General review of rainfall-runoff modeling: model calibration, data
4 775 assimilation, and uncertainty analysis. *Hydrological modelling and the water cycle*, 1-24.
5 776 Muleta, M., 2012. Model Performance Sensitivity to Objective Function during Automated Calibrations. *Journal*
6 777 *of Hydrologic Engineering*, 17, 756-767. doi:10.1061/(ASCE)HE.1943-5584.0000497
7
8 778 Nash, J.E. and Sutcliffe, J.V., 1970. River flow forecasting through conceptual models. Part 1. A discussion of
9 779 principles. *Journal of Hydrology*, 10, 282-290. doi:10.1016/0022-1694(70)90255-6
10 780 Noori, N. and Kalin, L., 2016. Coupling SWAT and ANN models for enhanced daily streamflow
11 781 prediction. *Journal of Hydrology*, 533, 141-151. doi:10.1016/j.jhydrol.2015.11.050
12 782 Noori, N., Kalin, L., and Lockaby, G., 2014. Predicting impacts of changing land use/cover on streamflow in
13 783 ungauged watersheds. *ASCE World Environmental & Water Resources Congress*, 1-5. doi:
14 784 10.1061/9780784413548.219
15
16 785 O'Brien, E.J., et al., 2015. A review of probabilistic methods of assessment of load effects in bridges. *Structural*
17 786 *Safety*, 53, 44-56. doi:10.1016/j.strusafe.2015.01.002
18 787 Olden, J.D. and Poff, N.L., 2003. Redundancy and the choice of hydrologic indices for characterizing streamflow
19 788 regimes. *River Research and Applications*, 19(2), 101-121. doi: 10.1002/rra.700
20
21 789 Palanisamy, B. and Workman, S.R., 2014. Observed hydrographs: on their ability to infer a time-invariant
22 790 hydrological transfer function for flow prediction in ungauged basins. *Hydrological Processes*, 28(3),
23 791 401-413. doi: 10.1002/hyp.9583
24
25 792 Pianosi, F., et al., 2016. Sensitivity analysis of environmental models: A systematic review with practical
26 793 workflow. *Environmental Modelling & Software*, 79(MAY), 214-232. doi: 10.1016/j.envsoft.2016.02.008
27 794 Rahman, K., et al., 2013. Streamflow modeling in a highly managed mountainous glacier watershed using SWAT:
28 795 the Upper Rhone River watershed case in Switzerland. *Water Resources Management*, 27(2), 323-339.
29 796 doi:10.1007/s11269-012-0188-9
30
31 797 Rajabi, M.M., Ataie-Ashtiani, B., and Simmons, C.T., 2015. Polynomial chaos expansions for uncertainty
32 798 propagation and moment independent sensitivity analysis of seawater intrusion simulations. *Journal of*
33 799 *Hydrology*, 520, 101-122. doi:10.1016/j.jhydrol.2014.11.020
34
35 800 Rao, A.R. and Han, J., 1987. Analysis of objective functions used in urban runoff models. *Advances in Water*
36 801 *Resources*, 10(4), 205-211. doi:10.1016/0309-1708(87)90030-3
37 802 Raposo, J.R., Molinero, J., and Dafonte, J., 2012. Parameterization and quantification of recharge in crystalline
38 803 fractured bedrocks in Galicia-Costa (NW Spain). *Hydrology and Earth System Sciences*, 16(6), 1667-1683.
39 804 doi:10.5194/hess-16-1667-2012
40
41 805 Razavi, T. and Coulibaly, P., 2012. Streamflow prediction in ungauged basins: review of regionalization
42 806 methods. *Journal of Hydrologic Engineering*, 18(8), 958-975. doi: 10.1061/(ASCE)HE.1943-5584.0000690
43 807 Ren, H., et al., 2016. Classification of hydrological parameter sensitivity and evaluation of parameter
44 808 transferability across 431 US MOPEX basins. *Journal of Hydrology*, 536, 92-108.
45 809 doi:10.1016/j.jhydrol.2016.02.042
46
47 810 Safeeq, M. and Fares, A., 2012. Hydrologic response of a Hawaiian watershed to future climate change
48 811 scenarios. *Hydrological Processes*, 26(18), 2745-2764. doi: 10.1002/hyp.8328
49 812 Saltelli, A., et al., 2004. *Sensitivity analysis in practice: a guide to assessing scientific models*. New York: Wiley.
50 813 Saltelli, A., Andres, T.H., and Homma, T., 1995. Sensitivity analysis of model output, Performance of the iterated
51 814 fractional factorial design method. *Computational Statistics & Data Analysis*, 20, 387-407.
52 815 doi:10.1016/0167-9473(95)92843-M
53
54 816 Saltelli, A., Chan, K., and Scott, E.M., 2000a. *Sensitivity Analysis*. New York: Wiley.
55 817 Saltelli, A., and Tarantola, S., 2002. On the relative importance of input factors in mathematical models: safety

- 1
2
3 818 assessment for nuclear waste disposal. *Journal of the American Statistical Association*, 97(459), 702-709.
4 819 <http://dx.doi.org/10.1198/016214502388618447>
- 5 820 Saltelli, A., Tarantola, S., and Campolongo, F., 2000b. Sensitivity analysis as an ingredient of modeling. *Statistical*
6 821 *Science*, 377-395. DOI: 10.1214/ss/1009213004
- 7
8 822 Sawicz, K., et al., 2011. Catchment classification: empirical analysis of hydrologic similarity based on catchment
9 823 function in the eastern USA. *Hydrology and Earth System Sciences*, 15(9), 2895-2911.
10 824 doi:10.5194/hess-15-2895-2011
- 11 825 Schaeffli, B. and Gupta, H.V., 2007. Do Nash values have value? *Hydrological Processes*, 21(15), 2075-2080.
12 826 doi: 10.1002/hyp.6825
- 13 827 Shafii, M. and Tolson, B.A., 2015. Optimizing hydrological consistency by incorporating hydrological signatures
14 828 into model calibration objectives. *Water Resources Research*, 51(5), 3796-3814. doi:
15 829 10.1002/2014WR016520
- 16 830 Shinohara, Y., et al., 2016. Effects of plant roots on the soil erosion rate under simulated rainfall with high kinetic
17 831 energy. *Hydrological Sciences Journal*, 61:13, 2435-2442, doi:10.1080/02626667.2015.1112904
- 18 832 Sobol', I.M., 2001. Global sensitivity indices for nonlinear mathematical models and their Monte Carlo estimates.
19 833 *Mathematics and Computers in Simulation*, 55(1-3), 271-280. doi:10.1016/S0378-4754(00)00270-6
- 20 834 Song, X., et al., 2015. Global sensitivity analysis in hydrological modeling: Review of concepts, methods,
21 835 theoretical framework, and applications. *Journal of Hydrology*, 523, 739-757.
22 836 doi:10.1016/j.jhydrol.2015.02.013
- 23 837 Steel, R.G.D. and Torrie, J.H., 1988. *Principles and Procedures of Statistics*. 2nd ed. New York: McGraw Hill.
- 24 838 Surfleet, C.G., Skaugset, A.E., and McDonnell, J.J., 2010. Uncertainty assessment of forest road modeling with
25 839 the Distributed Hydrology Soil Vegetation Model (DHSVM). *Canadian Journal of Forest Research*, 40(7),
26 840 1397-1409. doi:10.1139/X10-079
- 27 841 Tan, M.L., et al., 2015. Impacts of land-use and climate variability on hydrological components in the Johor River
28 842 basin, Malaysia. *Hydrological Sciences Journal*, 60:5, 873-889. doi:10.1080/02626667.2014.967246
- 29 843 Tang, Y., et al., 2007a. Advancing the identification and evaluation of distributed rainfall-runoff models using
30 844 global sensitivity analysis. *Water Resources Research*, 43(6). doi: 10.1029/2006WR005813
- 31 845 Tang, Y., et al., 2007b. Comparing sensitivity analysis methods to advance lumped watershed model
32 846 identification and evaluation. *Hydrology and Earth System Sciences Discussions*, 11(2), 793-817.
33 847 doi:10.5194/hess-11-793-2007
- 34 848 Thanapakpawin, P., et al., 2007. Effects of land use change on the hydrologic regime of the Mae Chaem river basin,
35 849 NW Thailand. *Journal of Hydrology*, 334(1-2), 215-230. doi: <http://dx.doi.org/10.1016/j.jhydrol.2006.10.012>
- 36 850 Vrugt, J.A., et al., 2003. Effective and efficient algorithm for multiobjective optimization of hydrologic
37 851 models. *Water Resources Research*, 39(8). doi: 10.1029/2002WR001746
- 38 852 Wagener, T., et al., 2001. A frame-work for development and application of hydrological models, *Hydrology and*
39 853 *Earth System Sciences Discussion*, 5(1): 13-26. doi:10.5194/hess-5-13-2001, 2001.
- 40 854 Wagener, T., et al., 2007. Catchment classification and hydrologic similarity. *Geography Compass*, 1(4), 901-931.
41 855 doi: 10.1111/j.1749-8198.2007.00039.x
- 42 856 Wang, Y. and Brubaker, K., 2015. Multi-objective model auto-calibration and reduced parameterization:
43 857 Exploiting gradient-based optimization tool for a hydrologic model. *Environmental Modelling & Software*, 70,
44 858 1-15. doi:10.1016/j.envsoft.2015.04.001
- 45 859 Westerberg, I.K. and McMillan, H.K., 2015. Uncertainty in hydrological signatures. *Hydrology and Earth System*
46 860 *Sciences*, 19(9), 3951-3968. doi:10.5194/hess-19-3951-2015
- 47 861 Wigmosta, M.S. and Burges, S.J., 1997. An adaptive modeling and monitoring approach to describe the

- 1
2
3 862 hydrologic behavior of small catchments. *Journal of Hydrology*, 202(1), 48-77.
4 863 doi:10.1016/S0022-1694(97)00057-7
5 864 Wigmosta, M.S., et al., 2002. The distributed hydrology soil vegetation model. *Mathematical models of small*
6 865 *watershed hydrology and applications*, 7-42.
7
8 866 Wigmosta, M.S. and Lettenmaier, D.P., 1999. A comparison of simplified methods for routing topographically
9 867 driven subsurface flow. *Water Resources Research*, 35(1), 255-264. doi: 10.1029/1998WR900017
10 868 Wigmosta, M.S. and Perkins, W.A., 2011. Simulating the effects of forest roads on watershed hydrology. *Land use*
11 869 *and watersheds: human influence on hydrology and geomorphology in urban and forest areas* 127-143.
12 870 doi: 10.1029/WS002p0127
13
14 871 Wigmosta, M.S., Vail, L.W., and Lettenmaier, D.P., 1994. A distributed hydrology-vegetation model for complex
15 872 terrain. *Water Resources Research*, 30(6), 1665-1679. doi: 10.1029/94WR00436
16 873 Winchell, M.F., et al., 2015. Using SWAT for sub-field identification of phosphorus critical source areas in a
17 874 saturation excess runoff region. *Hydrological Sciences Journal*, 60:5, 844-862. doi:
18 875 0.1080/02626667.2014.980262
19
20 876 Winsemius, H.C., et al., 2009. On the calibration of hydrological models in ungauged basins: A framework for
21 877 integrating hard and soft hydrological information. *Water Resources Research*, 45(12). doi:
22 878 10.1029/2009WR007706
23
24 879 Xu, Y. and Mynett, A.E., 2006. Application of uncertainty and sensitivity analysis in river basin management.
25 880 *Water Science and Technology*, 53(1), 41-49. doi: 10.2166/wst.2006.006
26 881 Xu, Y.P., et al., 2015. Coupling a Regional Climate Model and a Distributed Hydrological Model to Assess
27 882 Future Water Resources in Jinhua River Basin, East China. *Journal of Hydrologic Engineering*, 20(4),
28 883 04014054. doi: 10.1061/(ASCE)HE.1943-5584.0001007
29
30 884 Xu, Y.P., et al., 2014. Future potential evapotranspiration changes and contribution analysis in Zhejiang Province,
31 885 East China. *Journal of Geophysical Research-Atmospheres*, 119(5), 2174-2192. doi: 10.1002/2013JD021245
32 886 Xu, Y.P., et al., 2013. Impact of climate change on hydrology of upper reaches of Qiantang River Basin, East
33 887 China. *Journal of Hydrology*, 483, 51-60. doi:10.1016/j.jhydrol.2013.01.004
34
35 888 Yadav, M., Wagener, T., and Gupta, H., 2007. Regionalization of constraints on expected watershed response
36 889 behavior for improved predictions in ungauged basins. *Advances in Water Resources*, 30(8), 1756-1774.
37 890 doi:10.1016/j.advwatres.2007.01.005
38
39 891 Yan, J. and Haan, C.T., 1991. Multiobjective Parameter estimation for hydrologic models-Weighting of errors.
40 892 *Transactions of the ASAE*, 34(1), 135-141. doi: 10.13031/2013.31635
41 893 Ye, L., et al., 2014. Multi-objective optimization for construction of prediction interval of hydrological models
42 894 based on ensemble simulations. *Journal of Hydrology*, 519, 925-933. doi:10.1016/j.jhydrol.2014.08.026
43 895 Yilmaz, K.K., Gupta, H.V., and Wagener, T., 2008. A process-based diagnostic approach to model evaluation:
44 896 Application to the NWS distributed hydrologic model. *Water Resources Research*, 44(9). doi:
45 897 10.1029/2007WR006716
46
47 898 Zhan, C.S., et al., 2013. An efficient integrated approach for global sensitivity analysis of hydrological model
48 899 parameters. *Environmental Modelling & Software*, 41, 39-52. doi:10.1016/j.envsoft.2012.10.009
49 900 Zhang, C., Chu, J., and Fu, G., 2013. Sobol's sensitivity analysis for a distributed hydrological model of Yichun
50 901 River Basin, China. *Journal of Hydrology*, 480, 58-68. doi:10.1016/j.jhydrol.2012.12.005
51
52 902 Zhang, X., et al., 2013. Efficient multi-objective calibration of a computationally intensive hydrologic model
53 903 with parallel computing software in Python. *Environmental Modelling & Software*, 46, 208-218.
54 904 doi:10.1016/j.envsoft.2013.03.013
55 905

- 1
2
3 906 **Table 1.** Vegetation and soil classes and their percentages in Jinhua River Basin.
4 907 **Table 2.** Ranges, unit and abbreviation of constant, soil and vegetation parameters for ANOVA sensitivity analysis.
5 908 **Table 3.** Description of the six hydrological signatures used in the study.
6 909 **Table 4.** Ranges, number and abbreviation of parameters for Sobol's sensitivity analysis.
7 910 **Table 5.** Selected samples based on the *NE* value.
8 911 **Table 6.** Hydrological signatures of the observed and the simulated from selected samples and corresponding *P*-values.
9 912 **Table 7.** Selected samples for peak flow based on the *NS* value.
10
11 913
12 914
13 915 **Figure 1.** Methodology framework used in this study.
14 916 **Figure 2.** Location of the six stations used in the study.
15 917 **Figure 3.** DEM (digital elevation map) (a) soil distribution (b) and vegetation distribution (c) in Jinhua River Basin.
16 918 **Figure 4.** ANOVA parameter sensitivities based on the *NE* measure (F -value > 3).
17 919 **Figure 5.** Model performance in 1994, 1995 and 1996 (corresponding to moderate, wet and dry year, respectively) when the
18 920 value of *NE* (*NS*, E_{rel} and *NE* are 0.83, 0.81 and 0.82 respectively) is the maximum in ANOVA sensitivity analysis.
19 921 **Figure 6.** Sobol's total order sensitivity index based on the *NE* measure.
20 922 **Figure 7.** Interactions among sixteen parameters based on the *NE* measure.
21 923 **Figure 8.** Boxplot for *P*-value of hydrological signatures (*A1* (Mean annual runoff), *L1* (Low flow signature), *L2* (Base-flow
22 924 signature): and *H1* (Specific mean annual maximum flows)) of all samples in Sobol's sensitivity analysis.
23 925 **Figure 9.** Hydrological signature *DHI-4* for observed and simulated runoff from four selected samples as shown in Table 5.
24 926 **Figure 10.** Hydrological signature *DLI-4* for observed and simulated runoff from four selected samples as shown in Table 5.
25 927 **Figure 11.** Peak flow percentiles for observed and simulated runoff from samples whose *NE* > 0.7 in Sobol's sensitivity
26 928 analysis.
27 929 **Figure 12.** Peak flow percentiles for observed and simulated runoff from three selected samples as shown in Table 7.
28
29
30
31
32
33
34
35
36
37
38
39
40
41
42
43
44
45
46
47
48
49
50
51
52
53
54
55
56
57
58
59
60

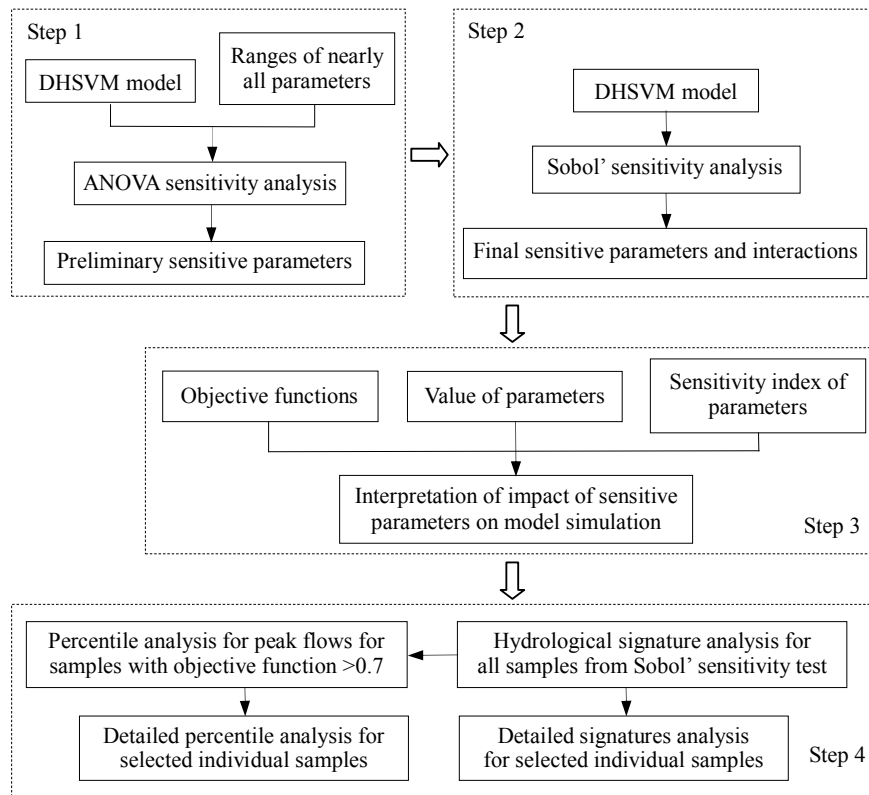


Figure 1. Methodology framework used in this study.

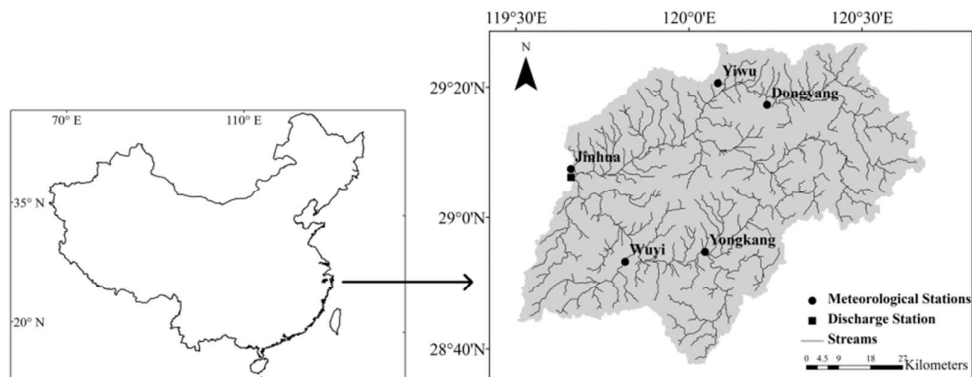


Figure 2. Location of the six stations used in the study.

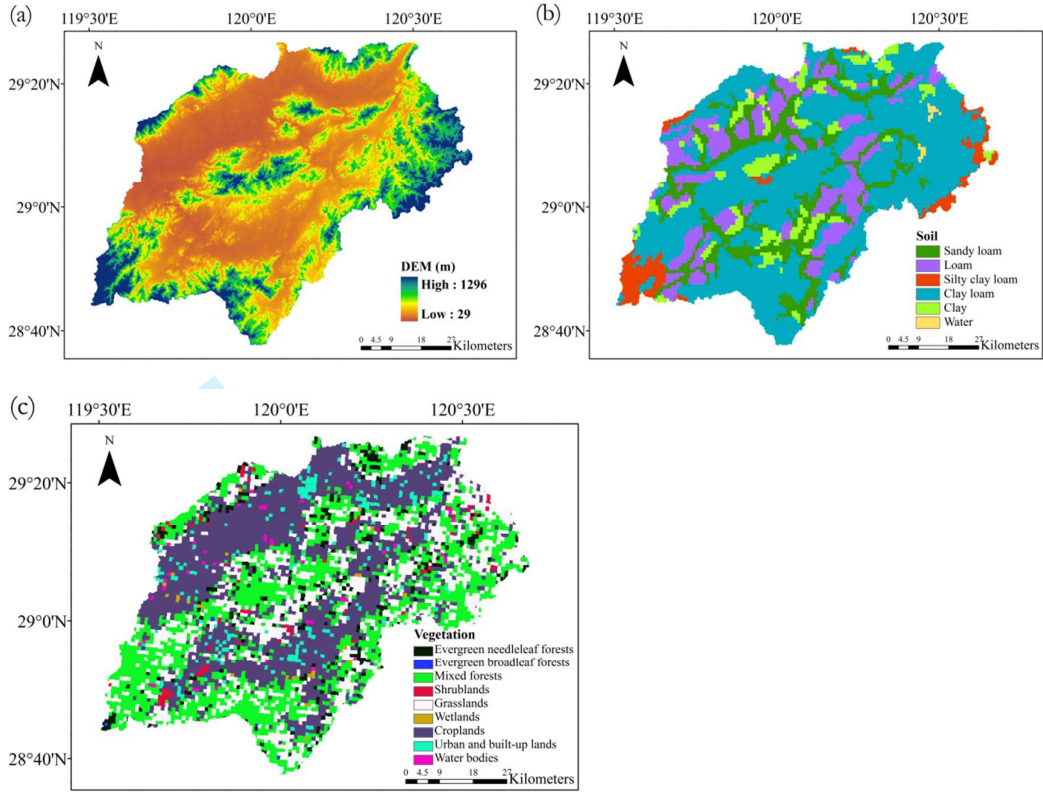


Figure 3. DEM (digital elevation map) (a) soil distribution (b) and vegetation distribution (c) in Jinhua River Basin.

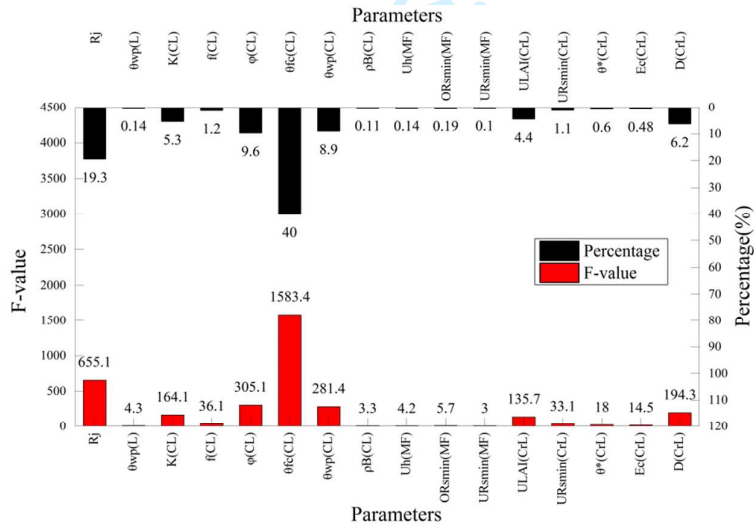


Figure 4. ANOVA parameter sensitivities based on the NE measure (F -value > 3).

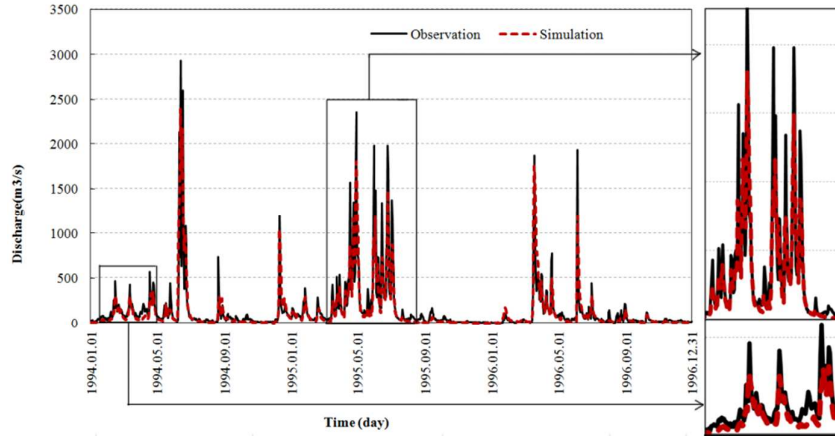


Figure 5. Model performance in 1994, 1995 and 1996 (corresponding to moderate, wet and dry year, respectively) when the value of NE (NS , $Erel$ and NE are 0.83, 0.81 and 0.82 respectively) is the maximum in ANOVA sensitivity analysis.

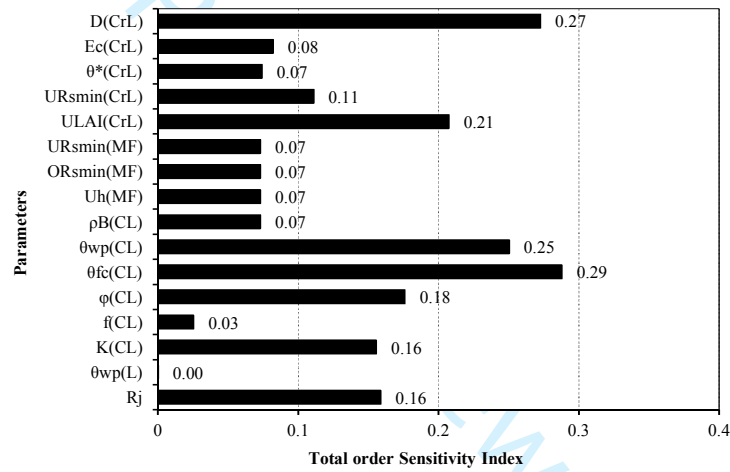


Figure 6. Sobol's total order sensitivity index based on the NE measure.

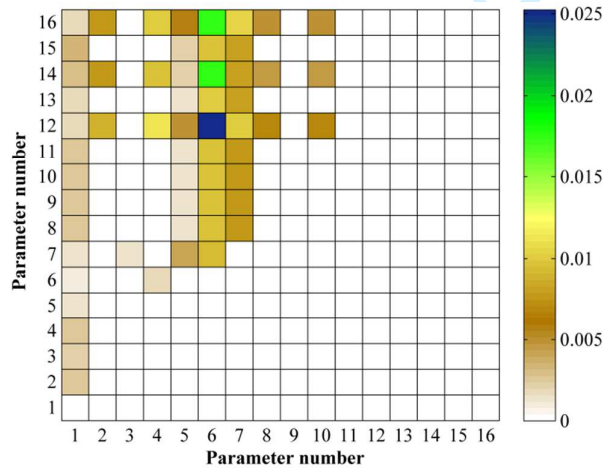


Figure 7. Interactions among sixteen parameters based on the NE measure.

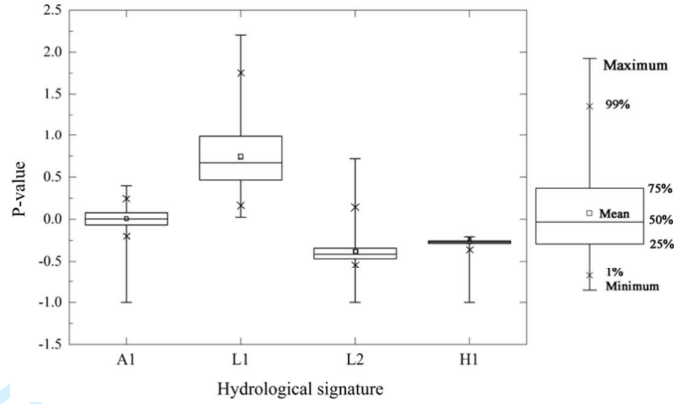


Figure 8. Boxplot for *P*-value of hydrological signatures (A1 (Mean annual runoff), L1 (Low flow signature), L2 (Base-flow signature); and H1 (Specific mean annual maximum flows)) of all samples in Sobol's sensitivity analysis.

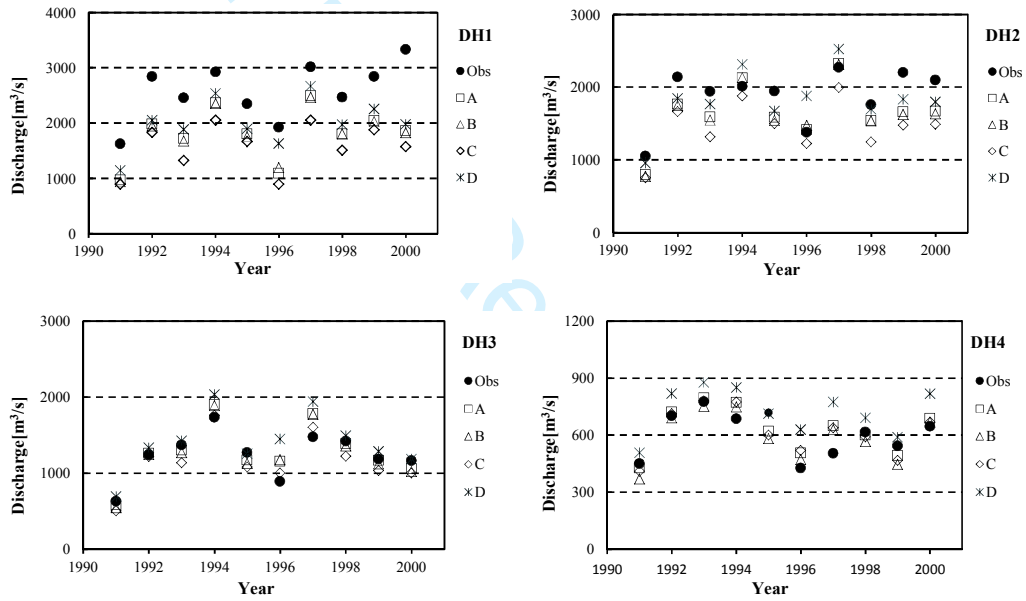


Figure 9. Hydrological signatures *DH1-4* for observed and simulated runoff from four selected samples as shown in Table 5.

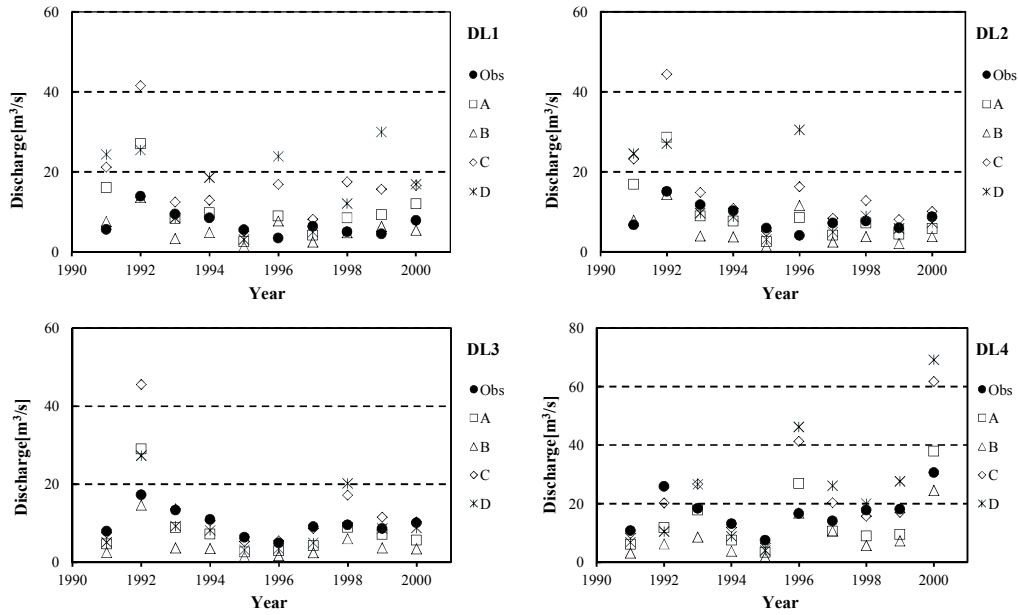


Figure 10. Hydrological signature $DLI-4$ for observed and simulated runoff from four selected samples as shown in Table 5.

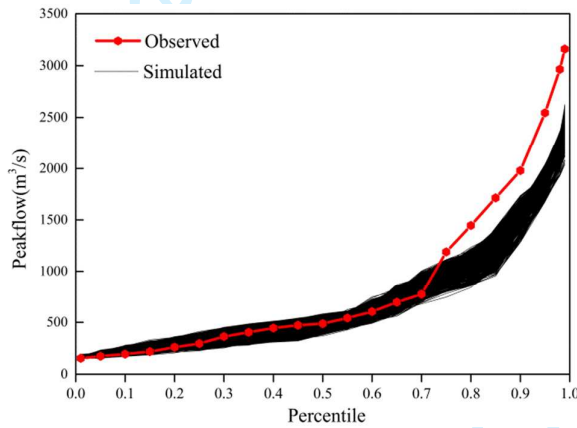


Figure 11. Peak flow percentiles for observed and simulated runoff from samples whose $NS > 0.7$ in Sobol's sensitivity analysis.

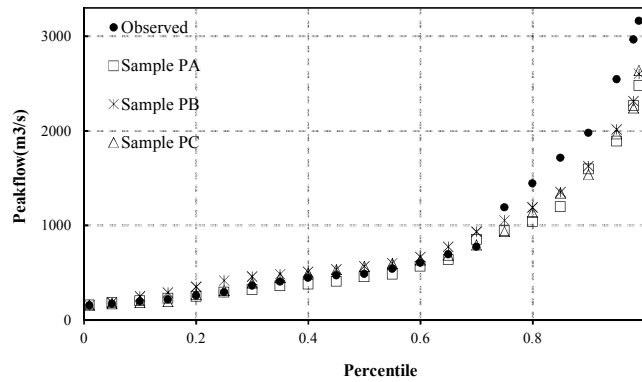


Figure 12. Peak flow percentiles for observed and simulated runoff from three selected samples as shown in Table 7.

Table 1. Vegetation and soil classes and their percentages in Jinhua River Basin.

Vegetation	Percentages	Vegetation	Percentages
Evergreen needleleaf forests	5.0	Water bodies	0.8
Evergreen broadleaf forests	0.1	Soil	Percentages
<i>Mixed forests</i>	<i>29.6</i>	<i>Sandy loam</i>	<i>16.5</i>
Shrublands	1.2	<i>Loam</i>	<i>15.8</i>
<i>Grasslands</i>	<i>22.9</i>	Silty clay loam	4.6
Wetlands	0.4	<i>Clay loam</i>	<i>55.4</i>
<i>Croplands</i>	<i>36.7</i>	Clay	7.3
Urban and built-up lands	3.3	Water	0.4

The italics represent soil/vegetation types whose area percentages are bigger than 10%.

Table 2. Ranges, unit and abbreviation of constant, soil and vegetation parameters for ANOVA sensitivity analysis.

Parameters	Abbrev.	Range	Parameters	Abbrev.	Range
Constant Parameters			Vegetation Parameters(Grasslands, GL; Croplands, CrL)		
Ground Roughness(m)	Zou	0.001–0.03	Understory Root Fraction	UFrjk	0–1
Rain Threshold(\square)	Tmin	-1–0	Understory Monthly LAI(m ² /m ²)	ULAI	0.3–3
Reference Height(m)	Zr	30–50	Understory Monthly Alb	Uaj	0.1–0.3
Rain LAI Multiplier(m)	Rj	0.00001–0.001	Understory Height(m)	Uh	0.3–2.5
Temperature Lapse Rate(\square /m)	Lt	-0.008– 0	Maximum Resistance(s/m)	Rsmax	300–1000
Vegetation Parameters(Mixed Forest, MF)			Understory Minimum Resistance(s/m)	URsmin	50–300
Fractional Coverage (m ² /m ²)	F	0.7–1	Soil Moisture Threshold(m ³ /m ³)	θ^*	0.1–0.35
Radiation Attenuation	Lb	0.1–0.3	Vapor Pressure Deficit(pa)	Ec	1000–6000
Trunk Space(m/m)	Rt	0.4–0.6	Rpc	Rpc	10–50
Aerodynamic Attenuation	Na	1.5–3.5	Root Zone Depths(m)	D	0.1–0.8
Overstory Root Fraction	OFrjk	0–1	Soil Parameters(Sandy Loam, SL; Loam, L; Clay Loam, CL)		
Overstory Monthly LAI(m ² /m ²)	OLAI	5–10	Lateral Conductivity (m/s)	K	0.00001–0.09
Overstory Monthly Alb	Oaj	0.1–0.3	Lateral Conductivity Exponential Decrease	f	1–4
Understory Root Fraction	UFrjk	0–1	Maximum Infiltration Rate (m/s)	Imax	0.00001–0.09
Understory Monthly LAI(m ² /m ²)	ULAI	0.3–3	Surface Albedo (m/s)	α	0.1–0.3
Understory Monthly Alb	Uaj	0.1–0.3	Porosity(m ³ /m ³)	φ	0.35–0.6
<i>Overstory Height(m)</i>	<i>Oh</i>	<i>10–25</i>	Pore Size Distribution	m	0.2–0.5
<i>Understory Height(m)</i>	<i>Uh</i>	<i>0.3–2.5</i>	Bubbling Pressure(m)	Ψ_b	0.1–0.76
Maximum Resistance(s/m)	Rsmax	2000–7000	Field Capacity(m ³ /m ³)	θ_{fc}	0.16–0.4
<i>Overstory Minimum Resistance(s/m)</i>	<i>ORsmin</i>	<i>300–800</i>	Wilting Point(m ³ /m ³)	θ_{wp}	0.05–0.25
<i>Understory Minimum Resistance(s/m)</i>	<i>URsmin</i>	<i>50–300</i>	Bulk Density(kg/ m ³)	ρ_B	1000–3000
Moisture Threshold(m ³ /m ³)	θ^*	0.1–0.35	Vertical Conductivity(m/s)	Ks	0.0001–0.5
Vapor Pressure Deficit(pa)	Ec	1000–60000	Thermal Conductivity (W/mK)	Kt	3–8
Rpc	Rpc	10–50	Thermal Capacity (J/m ³ K)	CV	1×10 ⁶ – 5×10 ⁶
Root Zone Depths(m)	D	0.1–0.8			

The abbreviations SL, L and CL in Table 2 represent sandy loam, loam and clay loam respectively. Similarly, MF, GL and CrL represent mixed forests, grasslands and croplands respectively. The italics represent parameters whose ranges for two vegetation stories are set separately.

Table 3. Description of the six hydrological signatures used in the study.

Conditions	Hydrological signature	Abbrev.	Unit	Definition
Average flow conditions	Mean annual runoff	<i>AI</i>	$m^3 s^{-1} km^{-2}$	Mean annual flow divided by catchment area
Low flow conditions	Low flow signature	<i>L1</i>	dimensionless	Mean of the lowest annual daily flow divided by mean annual daily flow averaged across all years
	Base-flow signature	<i>L2</i>	dimensionless	Seven-day minimum flow Divided by mean annual daily flows averaged across all years
Peak flow conditions	Specific mean annual maximum flows	<i>HI</i>	$m^3 s^{-1} km^{-2}$	Mean annual maximum flows divided by catchment area
Duration of flow events: Low flow conditions	Annual minimum of 1-/3-/7-/30-day means of daily runoff	<i>DL1-4</i>	$m^3 s^{-1}$	Magnitude of minimum annual flow of various duration, ranging from daily to monthly
Duration of flow events: Peak flow conditions	Annual maximum of 1-/3-/7-/30-day means of daily runoff	<i>DHI-4</i>	$m^3 s^{-1}$	Magnitude of maximum annual flow of various duration, ranging from daily to monthly

Table 4. Ranges, number and abbreviation of parameters for Sobol's sensitivity analysis.

Number	Parameters	Abbrev.	Ranges	Number	Parameters	Abbrev.	Ranges
1	Rain LAI Multiplier	Rj	0.00001-0.00	9	Understory Height(MF)	Uh(MF)	0.3-2.5
2	Wilting Point(L)	$\theta_{wp}(L)$	0.05-0.25	10	Overstory Minimum Resistance(MF)	ORsmin(MF)	300-800
3	Lateral Conductivity(CL)	K(CL)	0.00001-0.09	11	Understory Minimum Resistance(MF)	URsmin(MF)	50-300
4	Lateral (CL)	f(CL)	1-4	12	Understory Monthly LAI(CrL)	ULAI(CrL)	0.3-3
5	Porosity(CL)	$\phi(CL)$	0.35-0.6	13	Understory Minimum Resistance(CrL)	URsmin(CrL)	50-300
6	Field Capacity(CL)	$\theta_{fc}(CL)$	0.16-0.4	14	Soil Moisture Threshold(CrL)	$\theta'(CrL)$	0.1-0.35
7	Wilting Point(CL)	$\theta_{wp}(CL)$	0.05-0.25	15	Vapor Pressure Deficit(CrL)	Ec(CrL)	1000-6000
8	Bulk Density(CL)	$\rho_B(CL)$	1000-3000	16	Root Zone Depths(CrL)	D(CrL)	0.1-0.8

The italics represent parameters in the Sobol's sensitivity analysis whose ranges differ from ANOVA.

Table 5. Selected samples based on the *NE* value.

NE	0.85-0.88	0.80-0.85	0.75-0.80	0.70-0.75
Sample	Sample A(max NE)	Sample B	Sample C	Sample D

Table 6. Hydrological signatures of the observed and the simulated from selected samples and corresponding *P*-values.

Hydrological Signature	Obs	Sample A		Sample B		Sample C		Sample D	
		Sim	P	Sim	P	Sim	P	Sim	P
<i>AI</i>	9.34	8.44	-0.10	7.17	-0.23	9.43	0.01	11.3	0.21
<i>L1</i>	0.05	0.08	0.68	0.05	0.07	0.11	1.37	0.092	0.97
<i>L2</i>	0.23	0.15	-0.35	0.11	-0.54	0.25	0.09	0.13	-0.42
<i>HI</i>	0.44	0.31	-0.29	0.31	-0.30	0.27	-0.39	0.34	-0.22

Table 7. Selected samples for peak flow based on the *NS* value.

NS	0.80-0.85	0.75-0.80	0.70-0.75
Sample	Sample PA (max NS)	Sample PB	Sample PC

1
2
3
4
5
6
7
8
9
10
11
12
13
14
15
16
17
18
19
20
21
22
23
24
25
26
27
28
29
30
31
32
33
34
35
36
37
38
39
40
41
42
43
44
45
46
47
48
49
50
51
52
53
54
55
56
57
58
59
60

For Peer Review Only